



23 crustal ions (i.e., Ca^{2+} , Mg^{2+}), Na^+ , and Cl^- showed the highest concentrations in the semi-arid
24 regions and the coastal cities, respectively. The statistical methods confirmed that the mean
25 anthropogenic contribution ratios to SO_4^{2-} , F^- , NO_3^- , and NH_4^+ at a national scale were 46.12%,
26 71.02%, 79.10%, and 82.40%, respectively. However, Mg^{2+} (70.51%), K^+ (77.44%), and Ca^{2+}
27 (82.17%) were mostly originated from the crustal source. Both Na^+ (70.54%) and Cl^- (60.42%) were
28 closely linked to the sea-salt aerosols. On the basis of the stepwise regression (SR) analysis, it was
29 proposed that most of the secondary ions and F^- were closely related to gross industrial production
30 (GIP), total energy consumption (TEC), vehicle ownership, and N fertilizer use, but the crustal ions
31 (Ca^{2+} and K^+) were mainly controlled by the dust events. The influence of dust days, air temperature,
32 and wind speed on ions increased from Southeast China (SEC) to Central China, and then to
33 Northwest China (NWC), whereas the influence of socioeconomic factors on acid ions (SO_4^{2-} and
34 NO_3^-) displayed the higher value in East China.

35 **Keywords:** Water-soluble ions; precipitation; spatiotemporal variation; source identification; China

36 1. Introduction

37 Atmospheric wet deposition generally removes efficiently the aerosol particles and dissolved
38 gaseous pollutants from the atmosphere (Garland, 1978; Al-Khashman, 2005; Migliavacca et al.,
39 2005). However, in some regions with severe air pollution, the scavenging of substantial aerosol
40 particles alters the chemical compositions of precipitation and even aggravates the acid deposition
41 (Kuang et al., 2016). Some inorganic ions (i.e., SO_4^{2-} , NO_3^- , NH_4^+ , Ca^{2+}) play significant roles on
42 the terrestrial and aquatic ecosystem via wet deposition; for instance, leading to severe soil (lake)
43 acidification (alkalization), inhibiting the plant growth, and changing the regional climate (Liu et
44 al., 2011; Yan et al., 2010; Larssen and Carmichael, 2000; Larssen et al., 1999). In the past decades,



45 China has been suffered from the severe air pollution along with the population growth and
46 industrialization (Liu et al., 2016a). Therefore, the investigation of the wet deposition status of
47 inorganic ions is of great interest to the public and policy makers (Négrel et al., 2007).

48 A large amount of studies mainly focused on the spatiotemporal variation of the S and N
49 deposition around the world due to their adversely ecological effects in the past decades (Gerson et
50 al., 2016; Clemens 2006; Zhang et al., 2010). Okuda et al. (2005) showed that the SO_4^{2-}
51 concentration in the precipitation exhibited a slight decrease coupling with the decrease of the SO_2
52 concentration in Tokyo during 1990-2012. Hunová et al. (2014) reported that the averagely S
53 deposition flux decreased from 181 kg/ha/year to 100 kg/ha/year in Czech during 1995 and 2011 on
54 the basis of the data in 15 cities. Du et al. (2012) estimated that the wet deposition flux of inorganic
55 nitrogen reached 3.5 kg N/ha/year according to the average of 151 monitoring in the United States
56 during 1985-2012, which were significantly lower than that of China during the same period (11.11-
57 13.87 kg/ha/yr) (Jia et al., 2014).

58 Many researches about the S and N deposition have been extensively performed to date in China
59 in the recent years (Jia et al., 2014; Xu et al., 2015). In the past decades, the anthropogenic emissions
60 of SO_2 , NO_2 , and NH_3 displayed the remarkable increase along with the dramatic increase of fossil
61 fuel and fertilizer consumption in China (Jia et al., 2014; Kuribayashi et al., 2012). It was well
62 documented that the gaseous precursors containing S and N could be transformed into sulfates
63 (SO_4^{2-}), nitrates (NO_3^-), and ammonium (NH_4^+) during ageing in the atmosphere, thereby
64 contributing to the formation of airborne fine particles, of which were considered to be the main
65 reason for the persistent fog and haze pollution in China (Wang et al., 2016a; Qiao et al., 2015). At
66 a city level, Huang et al. (2008) observed that the wet deposition fluxes of SO_4^{2-} , NH_4^+ , and Ca^{2+}



67 displayed the slight decrease from 1986 to 2006 in the urban of Shenzhen, whereas the wet
68 deposition of NO_3^- increased rapidly during the same period. Very recently, Pu et al. (2017) reported
69 that the SO_4^{2-} concentration in the wet deposition of Shangdianzi (a regional background station of
70 Beijing) showed slight decrease during 2003-2014, but the NO_3^- concentration showed an opposite
71 trend. At a regional scale, Pan et al. (2013) observed that the highest S wet deposition was
72 concentrated in the urban and industrial region of Tianjin among of ten sites of North China (NC).
73 Song et al. (2017) suggested that the bulk deposition fluxes were in the order of Chengdu (urban) >
74 Yanting (agricultural area) > Gongga mountain (natural reserve). At a national scale, Jia et al. (2014)
75 firstly found that the wet deposition of N in Southeast China (SEC) showed a significant decrease,
76 whereas it increased slightly in the western of China on the foundation of the data (620 monitoring
77 sites) collected from 120 cities across China during 1990 and 2010. Following this work, Liu et al.
78 (2016) further observed that the serious S deposition (79 monitoring sites) on SEC and Southwest
79 China (SWC). In these studies, the spatial distributions of both S and N were determined using the
80 spatial interpolation method, which generally required substantial monitoring sites (city > 150, and
81 monitoring site > 300). However, these conclusions were obtained based on a small quantity of
82 monitoring sites, which increased the uncertainties of the results. Meanwhile, the monitoring sites
83 in these studies were mainly located on some remote regions such as mountain or rural site rather
84 than the mixture of urban, suburban, and rural sites, which cannot accurately reflect the spatial
85 variations of inorganic ions in China. Moreover, the spatiotemporal variations of other inorganic
86 ions (i.e., K^+ , Ca^+ , Mg^{2+}) remained unclear to date, which were also linked to the acid deposition,
87 as well as the haze pollution in China (Mikhailova et al., 2013; Aloisi et al., 2017; Müller et al.,
88 2015).



89 Based on these field measurements, the ion levels in the deposition across China were believed
90 to be underestimated due to the few ion species measured by previous studies (Liu et al., 2016a),
91 which was closely associated with various emission sources (Kuang et al., 2016). Thus, the source
92 identification should be performed to assess accurately their contributions to the wet deposition
93 (Larssen et al., 1999). Liu et al. (2015b) identified that the Cl^- and NH_4^+ in the precipitation of Tibet
94 were both originated from the marine and crustal source using the geochemical index method. On
95 the basis of the positive matrix factorization (PMF) model, Qiao et al. (2015) showed that fossil fuel
96 combustion and agriculture were the main sources of SO_4^{2-} and NO_3^- in Jiuzhaigou (Sichuan
97 province). In a newly work reported by Leng et al. (2018), they supposed that the combustion of
98 fossil fuels, domestic sewages, and fertilizers were the main sources of the N-bearing ions on the
99 basis of the N isotope analysis. To date, some methods, including geochemical index method,
100 multivariate analyses, and isotope signatures have been utilized to identify the anthropogenic versus
101 natural sources of the inorganic ions in the precipitation. However, these methods suffered from
102 some weaknesses from different standpoints (AlKhatib and Eisenhauer 2017; Shi et al., 2014). For
103 instance, the geochemical index methods cannot estimate the contribution ratios of multiple sources
104 to Ca^{2+} and Na^+ at a spatial scale (Liu et al., 2015b). Despite the advances of multivariate analyses
105 lowering the associated uncertainties, the multi-collinearity still disturbed the predictions of these
106 models (Shi et al., 2014). The isotope signature method was costly and complex, especially for the
107 unconventional stable isotopes (i.e., K, Ca) (AlKhatib and Eisenhauer 2017), which restricted its
108 application at a large scale. Therefore, multiple source apportionment methods should be combined
109 in order to enhance the reliability of the results. Liu et al. (2015) also demonstrated that the
110 geochemical index method coupled with multiple statistics decreased the uncertainties of results.



111 Apart from the source apportionment, the key factor identification for the ions in the wet
112 deposition is also of great importance to reduce the acid deposition. At an early study, Singh and
113 Agrawal (2008) revealed that the significant increase of vehicle emissions contributed to the
114 accumulation of NO₂, which might be an important precursor of acid rain. Allen et al. (2015)
115 observed that some inland cities in arid and semi-arid regions were generally subjected to dust
116 events, which could increase the Ca²⁺ and K⁺ concentrations in the wet deposition. Following this
117 work, Yu et al. (2017a) found that considerable energy consumption, gross domestic production
118 (GDP), and emitted substantial pollutants made China as major regions of acid rain around the world
119 using path analysis and correlation analysis. However, these researches only assessed the limited
120 factors for the inorganic ions in the wet deposition (Yu et al., 2016; Yu et al., 2017a), ignoring the
121 contributions of other socioeconomic and natural factors. Moreover, these researches mainly
122 focused the whole effects of the influential factors on inorganic ions at a national scale, while they
123 did not consider the spatial heterogeneity of the influential factors, resulting possibly in the great
124 deviation of the inorganic ions in the wet deposition for the different regions.

125 Here, the data of nine water-soluble ions in the precipitation including Ca²⁺, Cl⁻, F⁻, K⁺, Mg²⁺,
126 Na⁺, NH₄⁺, NO₃⁻, and SO₄²⁻ in the 320 cities across the whole China were collected during 2011-
127 2016 to examine the characteristics of the main water-soluble ions in the precipitation. Specifically,
128 the objectives of our study were (1) to reveal the spatiotemporal patterns of water-soluble ions in
129 the precipitation recently in China at a national scale; (2) to identify quantitatively the source of the
130 water-soluble ions in the precipitation based on the multiple statistical methods; and (3) to seek out
131 the key factors for the inorganic ions at a spatial scale. This study supplied the systematical data for
132 comprehensive understanding on the inorganic composition in the precipitation based on the long-



133 term field measurement, at a national scale (the 1282 monitoring sites distributed in the 320 cities
134 across the whole China), which was beneficial to the implementation of appropriate strategies to
135 promote environmental protection in China.

136 **2. Materials and methods**

137 2.1 Site description

138 The spatial distribution of field stations in National Acid Deposition Monitoring Network
139 (NADMN) is illustrated in Fig. 1. The selected 1282 monitoring sites are distributed in the 320 cities
140 across 31 provinces. These cities are classified into Northeast China (NEC), NC, SEC, Northwest
141 China (NWC), and Southwest China (SWC) (Tab. S1). Both of NEC and NC show typical
142 temperature monsoon climate, while SEC presents the subtropical monsoon climate. The SWC
143 region suffers from the combined effects of subtropical monsoon climate and tropical monsoon
144 climate. NWC suffers from the temperate continental climate and displays minor rainfall amount.
145 NEC and NC are filled with temperate deciduous forest, whereas SEC is mainly occupied by the
146 subtropical evergreen forest. The subtropical evergreen forest and tropical evergreen forest spread
147 out the SWC region. The NWC is generally filled with expansive grasslands and desert. The
148 latitudes and longitudes of all of 1282 monitoring sites range from 18.25 to 50.78° N, and from 79.57
149 to 129.25° E, respectively. Annual mean rainfall ranges from 10 to 1853 mm and the annual mean
150 air temperature varies between -6.9 and 24.3 °C. The monitoring sites were designed as a mixture
151 of urban and background sites. Most of these sites are concentrated in urban region, and a few of
152 sites in suburban and rural areas are considered as the background sites.

153 2.2 Sampling and chemical analysis

154 The real-time precipitation was collected by monitors in the field stations as a routine procedure



155 of NADMN. Samples from each monitoring site were collected using wet deposition automatic
156 collectors (diameter 30 cm) installed at 1.5 m above ground level. The cover of the collection
157 instrument opened automatically without delay when the precipitation sensor was activated and
158 closed automatically when precipitation ceased and no water remained on the sensor surface. After
159 the sampling, the pH and EC values of the samples were measured immediately. The sample pH
160 was measured using a pH meter (MP-6p, HACH, USA) at 20–25°C. The EC value of the
161 precipitation samples was determined by an EC meter (CyberScan, CON1500, USA). After the
162 analysis of pH and EC, all of the samples were contained in the pre-cleaned polyethylene plastic
163 bottles at -18°C in order to prevent the possible transformation by microbes. All of the plastic
164 buckets and the polyethylene plastic bottles were cleaned with deionized water for more than three
165 times and then air-dried in clean room prior to use.

166 All of the precipitation samples were used to analyze the concentrations of the water-soluble
167 ions including NO_3^- , Cl^- , Ca^{2+} , K^+ , F^- , NH_4^+ , Mg^{2+} , SO_4^{2-} , and Na^+ . The microporous membranes
168 (0.45 μm) were employed to remove all of insoluble particulates ($< 0.45\mu\text{m}$) from the precipitation
169 samples before the analysis. The ion concentrations were determined through ion chromatography
170 (Dionex ICS-900) equipped with a conductivity detector (ASRS-ULTRA). The CS12A column and
171 AS11-HC column were applied to determine the cations and anions, respectively. Each sample was
172 measured for more than three times and the relative standard deviation was less than 5% for each
173 ion. Analysis of the blank samples once a month confirmed that the cross contamination in the
174 present research was negligible. For each ion, the analysis of simulated precipitation suggested that
175 the relative bias was lower than 10%.

176 2.3 Data calculation



177 The monthly and annual volume-weighted mean (VWM) concentrations were calculated based
 178 on the concentrations of specific ions and precipitation. The monthly and annual VWM
 179 concentrations were obtained as follows:

$$180 \quad C_x = \frac{\sum_{i=1}^n (C_i(x) \times P_i)}{\sum_{i=1}^n P_i} \quad (1)$$

181 where C_x denoted the monthly and annual VWM concentration of the given ion; $C_i(x)$ was the
 182 concentration of the given ion in the precipitation ($\mu\text{eq/L}$); P_i was the precipitation in individual
 183 sample. The monthly and annual VWM pH values were obtained based on the corresponding VWM
 184 concentrations of H^+ via Eq. (1).

185 The wet deposition flux of the given ion was calculated using the following Eq. (2)

$$186 \quad D_w = P_t C_w / 100 \quad (2)$$

187 where D_w was the wet deposition flux of the given ion (kg N ha^{-1}); P_t was the total amount of the
 188 precipitation events (mm); C_w was the VWM concentration of each ion (mg/L); and 100 was a unit
 189 conversion factor.

190 In order to obtain the contributions of various alkaline species to acid neutralization in the
 191 precipitation, the neutralization factor (NF) was calculated using the following Eq. (3)-(5)
 192 (Kulshrestha et al., 1995):

$$193 \quad NF_{\text{NH}_4^+} = \frac{\text{NH}_4^+}{\text{NO}_3^- + \text{SO}_4^{2-}} \quad (3)$$

$$194 \quad NF_{\text{Ca}^{2+}} = \frac{\text{Ca}^{2+}}{\text{NO}_3^- + \text{SO}_4^{2-}} \quad (4)$$

$$195 \quad NF_{\text{Mg}^{2+}} = \frac{\text{Mg}^{2+}}{\text{NO}_3^- + \text{SO}_4^{2-}} \quad (5)$$



196 2.4 Source apportionment of ionic species in wet deposition

197 The enrichment factor (EF) has been widely applied to estimate the contribution ratios of the
198 various sources to the major ions in the previous studies (Lawson and Winchester 1979; Cao et al.,
199 2009; Lu et al., 2011). In the present study, an ion EF in the precipitation relative to the ion in the
200 sea was calculated using Na as a reference element as follows:

$$201 \quad EF_{sea} = \frac{(X / Na^+)_{precipitation}}{(X / Na^+)_{sea}} \quad (6)$$

202 where EF_{sea} was the enrichment indicator of a given ion in the precipitation relative to the ion in the
203 sea; X was the ion in the precipitation; $(X/Na^+)_{precipitation}$ represented the ratio of components in the
204 precipitation; $(X/Na^+)_{sea}$ denoted the ratio of components in the sea (Keene et al., 1986; Turekian,
205 1968).

206 The EF value of an ion in the precipitation relative to the corresponding ion in the soil was
207 calculated following Eq. (7):

$$208 \quad EF_{soil} = \frac{(X / Ca^{2+})_{precipitation}}{(X / Ca^{2+})_{soil}} \quad (7)$$

209 where EF_{soil} represented the EF value of an ion in the precipitation relative to the corresponding ion
210 in the soil; X denoted an ion in the precipitation; $(X/Ca^{2+})_{precipitation}$ was the ratio of components in
211 the precipitation; $(X/Ca^{2+})_{soil}$ denoted the ratio of components in the soil (Wei et al., 1991; Wei et al.,
212 1992; Shi et al., 1996; Zhang et al., 2012; Chen et al., 1992).

213 In order to quantify the anthropogenic source versus natural one of ionic species in the
214 precipitation. The fractions of anthropogenic, marine, and crustal source contributed to the ions in
215 the precipitation were calculated as follows:



$$216 \quad SSF = \frac{(X / Na^+)_{sea}}{(X / Na^+)_{precipitation}} \times 100\% \quad (8)$$

$$217 \quad CF = \frac{(X / Ca^{2+})_{soil}}{(X / Ca^{2+})_{rain}} \times 100\% \quad (9)$$

$$218 \quad AF = 100\% - SSF - CF \quad (10)$$

219 where *SSF* represented the fraction of sea salt; *CF* denoted the crustal contribution; and *AF* denoted
220 the anthropogenic fraction. *SSF* was recalculated as the difference between 1 and *CF* when *SSF* was
221 greater than 1; *CF* was recalculated as the difference between 1 and *SSF* when *CF* was higher than
222 1.

223 FA has been widely employed to determine the contribution ratios of natural and anthropogenic
224 source to ionic species in the precipitation. First of all, FA was applied to reduce the dimension of
225 original variables (measured ion concentrations in samples) and to extract a small number of
226 principal components to analyze the relationships among the observed variables. All of the factors
227 with eigenvalues over 1 were extracted based on the Kaiser-Meyer-Olkin (KMO) test and the
228 Bartlett's test of sphericity, and were rotated using the Varimax method. The FA factor scores and
229 each ion concentration were treated as independent and dependent variables, respectively. The
230 resultant regression coefficients were employed to convert the absolute factor scores and then to
231 calculate the contribution of each PC source (Luo et al., 2015).

232 2.5 The geographical weight regression (GWR) method

233 Although the relationships between the independent variables and the dependent variables could
234 be calculated using correlation analysis and multiple linear regression analysis (MLR), these
235 methods cannot show the spatial variability of regression coefficients. Thus, the GWR method was
236 applied to generate the local regression coefficients for each city, which were then mapped to display



237 the spatial variability. Local regression coefficients were obtained using weighted least squares with
238 the following weighting function (Brunsdon et al., 1996):

$$239 \quad \beta(u_i, v_i) = (X^T W(u_i, v_i) X)^{-1} X^T W(u_i, v_i) Y \quad (11)$$

240 where $\beta(u_i, v_i)$ represented the local regression coefficient at city i ; X was the matrix of the
241 influential factors; Y denoted the matrix of the wet deposition fluxes of the water-soluble ions; and
242 $W(u_i, v_i)$ was an n order matrix that the diagonal elements were the spatial weighting of the influential
243 factors. The spatial weight function was calculated via the exponential distance decay form:

$$244 \quad W(u_i, v_i) = \exp(-d^2(u_i, v_i) / b^2) \quad (12)$$

245 where $d(u_i, v_i)$ represented the distance between the location i and j , and b was the kernel bandwidth.

246 2.6 Data source and statistical analysis

247 The data of GDP, gross industrial production (GIP), N fertilizer use, vehicle ownership, urban
248 green space (UGS) during 2011-2016 were collected from China City Statistical Book. Total energy
249 consumption (TEC) during the period were obtained from China Energy Statistical Yearbook, which
250 consisted of the consumption of coal, crude oil, and natural gas. The daily meteorological factors
251 including precipitation, maximum and minimum air temperature, wind speed, air pressure, relative
252 humidity (RH) during 2011-2016 were collected from China Meteorological Data Network. The
253 daily visibility data during 2011-2016 was collected from National Centers for Environmental
254 Prediction (NCEP). The data of dust days were calculated based on the horizon visibility data. The
255 days with the visibility lower than 1 km were treated as the dust days. The daily data of PM_{2.5}, PM₁₀,
256 SO₂, and NO₂ were downloaded from the National Environmental Monitoring Platform
257 (<https://www.aqistudy.cn/historydata/>). These data at a national scale were open access since
258 January 2014. To match the meteorological data at a national scale, the data of air pollutants during



259 2014-2016 were applied to investigate the relationships of the water-soluble ions, meteorological
260 factors, and the air pollutants in the atmosphere (Tab. S2). In addition, the SR analysis was employed
261 to determine the key factors regulating the wet deposition fluxes of the water-soluble ions. All of
262 the statistical analysis were performed by the software package of ArcGIS 10.2, SPSS 21.0, and
263 Origin 8.0 for Windows 10.

264 **3 Results and discussion**

265 3.1 The pH and EC values in the precipitation

266 To obtain the preliminary knowledge about the precipitation characteristics, the basic
267 physiochemical properties including pH and EC of the precipitation samples are presented in Fig.
268 2. The annually pH during 2011 and 2016 ranged from 5.45 ± 0.27 (mean \pm standard deviation) to
269 5.94 ± 0.46 and the mean value was 5.76 (Fig. 2a). Seinfeld (1986) estimated that the precipitation
270 with pH lower than 5.60 was considered as acid rain because the pH value of natural water in
271 equilibrium with atmospheric CO_2 was 5.60. However, the CO_2 level has been increasing in recent
272 years and thus the equilibrium pH has changed (McGlade and Ekins 2015) Therefore, the average
273 CO_2 concentration during 2011-2016 (396.83 ppm) around the world was applied to the present
274 study (<http://www.ipcc.ch/>). The ionization equation of CO_2 include $\text{CO}_2 + \text{H}_2\text{O} = \text{H}_2\text{CO}_3$ and
275 $\text{H}_2\text{CO}_3 = \text{HCO}_3^- + \text{H}^+$. The dissociation constant of two equations are 3.47×10^{-2} (K_0) and 4.4×10^{-7} (K_1),
276 respectively. The $(c(\text{H}^+))^2 = K_0 \times K_1 \times P_{\text{CO}_2} = 6.06 \times 10^{-12}$. Therefore, the equilibrium pH was 5.61,
277 which was slightly higher than the current value (pH = 5.60). Herein, 41% of the samples during
278 the measurement showed the pH value below 5.61. Compared with the pH value of the precipitation
279 during 1980-2000 (Wang and Xu 2009), the pH value of the precipitation showed a remarkable
280 increase in recent years. For instance, the pH value in the precipitation of SWC increased from 3.5-



281 4.0 (the mean value of 1980-2000) to 5.87 during 2011-2016. Although some cities in Hunan and
282 Hubei province (e.g., Chengzhou, Erzhou) still suffered from the severe acid deposition, the mean
283 pH values (4.46) of the two provinces during 2011-2016 were slightly higher than those in 1980-
284 2000 (3.5-4.0). It was well known that precipitation pH was associated with the SO₂ and NO_x
285 emissions (Pu et al., 2017). Due to the implementation of SO₂ control measurements since the 11th
286 Five-year Plan, the SO₂ column concentration over China displayed a marked decrease after 2007
287 based on Global Ozone Monitoring Experiment (GOME), reported by Gottwald and Bovensmann
288 (2011). Based on the bottom-up method, Liu et al. (2010) also supposed that SO₂ emission began to
289 decrease since 2007 (Lu et al., 2010), in good agreement with the results obtained from the remote
290 sensing. Besides, nearly all of the power plants built newly and the in-use plants have been required
291 to be equipped with advanced selective catalytic reduction (SCR) or selective non-catalytic
292 reduction (SNCR) since 2010 (Tian et al., 2013; Lu et al., 2011), resulting in a gradual decrease of
293 the NO_x emission after 2010 (China Statistical Yearbook,
294 <http://data.stats.gov.cn/easyquery.htm?cn=C01>). Based on the result of correlation analysis (Tab.
295 S2), the pH value showed the significantly negative correlation with SO₂ and NO₂ in the ambient
296 air especially with the increased RH. Thus, it could be proposed that the pH value of the
297 precipitation in most of the regions of China during 2011 and 2016 were significantly higher than
298 those before 2000 due to the decreases of the SO₂ and NO_x emissions.

299 The pH value in the precipitation at a national scale exhibited significantly seasonal variation
300 with the highest value in summer (6.57), followed by autumn (5.64), spring (5.49), and the lowest
301 one in winter (5.32) (Fig. 2b). The seasonal variation of pH values in wet deposition was supposed
302 to be linked with the wash-out effect of precipitation on atmospheric particular matters (Xing et al.,



2017), which was supported by the positive relevance between pH and precipitation ($p < 0.01$). Besides, the scavenging atmospheric SO_2 by precipitation may also play an important role in the seasonal variation of the pH values (Wu and Han, 2015). The atmospheric SO_2 concentration was the lowest in summer and the highest in winter. The highest atmospheric SO_2 and sulfate concentrations in winter of the north part of China were partially ascribed to the intensive domestic coal combustion for heating (Liu et al., 2016b; Liu et al., 2017).

At a spatial scale across the whole China (Fig. 3a), the pH value of the precipitation presented a gradual increase from SEC to NC and NWC. The relatively low pH values in the precipitation were usually observed in YRD (i.e., Huzhou, Ningbo, and Shanghai), Hunan province (i.e., Changde, Changsha, and Loudi), Hubei province (i.e., Wuhan), and Jiangxi province (i.e., Nanchang, Yichun, and Jingdezhen), but the relatively high pH values occurred in NC and NWC, especially in Xinjiang autonomous region (i.e., Changji, Altai, Urumqi and Aksu). Among of the 320 cities, the lowest one and the highest one were located in Huzhou, (3.20, Zhejiang province), and Altai, (6.82, Xinjiang autonomous region), respectively (Fig. 3). Compared with high acidity in some cities of SEC, the acidity of the precipitation in many cities of NC could be largely neutralized by some alkaline ions because the saline-alkali soils were widely distributed in NC (Wang et al., 2014). Some city atmosphere (i.e., Urumqi and Altay) in Xinjiang autonomous region were frequently attacked by local continental dust particles, diluting the precipitation acidity (Rao et al., 2015).

The annually mean EC varied from $10.18 \pm 3.21 \mu\text{S cm}^{-1}$ to $13.33 \pm 3.75 \mu\text{S cm}^{-1}$ during the period (Fig. 2a). The EC value was mainly affected by total water-soluble ions in the precipitation and rainfall amount, of which indirectly reflected the cleanliness of the precipitation and the air pollution status. The decrease of EC in recent years suggested that air pollution in China has been



325 mitigated due to the implementation of special air pollution control measures (Wang et al., 2017;
326 Yang et al., 2016). The EC value also presented distinctly seasonal variation and showed the highest
327 value in spring (Fig. 2c), followed by ones in summer and autumn, and the lowest one in winter,
328 which was apparently different from the seasonal pH variation. Among all of the inorganic ions,
329 only Ca^{2+} displayed notable relationship with EC ($p < 0.01$). It was supposed that many crustal ions
330 such as Ca^{2+} could be lifted up and transported to East China by frequent dust storms in spring and
331 summer, thereby leading to the high EC value in the precipitation (Fu et al., 2014). The mean EC
332 value exhibited a significantly spatial variation with the higher ones in Shizuishan ($36.60 \mu\text{S cm}^{-1}$)
333 and Yinchuan ($24.79 \mu\text{S cm}^{-1}$) (Ningxia autonomous region), Wuwei ($60.01 \mu\text{S cm}^{-1}$) (Gansu
334 province), Edors ($28.72 \mu\text{S cm}^{-1}$) (Inner Mongolia autonomous region), and Aksu ($22.06 \mu\text{S cm}^{-1}$)
335 (Xinjiang autonomous region) and the lower one in some remote regions such as Lhasa ($3.42 \mu\text{S cm}^{-1}$)
336 (Tibet autonomous region), Aba ($2.20 \mu\text{S cm}^{-1}$) (Sichuan province) and Diqing ($2.46 \mu\text{S cm}^{-1}$) (Yunan
337 province) (Fig. 3b). The lowest and highest EC were observed in Aba ($2.20 \mu\text{S cm}^{-1}$) and Wuwei
338 ($60.01 \mu\text{S cm}^{-1}$), respectively (Fig. 3). The cities in the western and northern of Sichuan province,
339 and the southern of Tibet autonomous region presented the lower EC values due to the sparse
340 population and minimal industrial activity. Although TB has received the effects of the industrial
341 emissions and biomass burning from South Asia via a long-range atmospheric transport, most of the
342 pollutants tended to be deposited on the South of Himalayas except persistent organic pollutants
343 (POPs) (Yang et al., 2016b; Dong et al., 2017). The cities with higher EC was generally close to the
344 Taklamakan and Gobi deserts. Strong winds in these deserts stirred a large amount of dusts, and
345 then caused many dust events, resulting in high loading of Ca^{2+} and Mg^{2+} (Wang et al., 2016d). The
346 positive relationship between wind speed and EC also revealed that strong wind promoted the



347 accumulation of crustal ions over China (Tab. S2).

348 3.2 Chemical composition in the precipitation

349 3.2.1 The inter-annual variation of the water-soluble ions

350 The inter-annual variation of the ionic constituents of the precipitation in China during 2011-2016
351 are summarized in Fig. 4. The concentrations of Na^+ , NO_3^- , and SO_4^{2-} increased from 7.26 ± 2.51 ,
352 11.56 ± 3.71 , and 33.73 ± 7.59 $\mu\text{eq/L}$ to 11.04 ± 4.64 , 13.59 ± 2.63 , and 41.95 ± 8.64 $\mu\text{eq/L}$ during
353 2011 and 2014, respectively (Fig. 4a). However, Na^+ , NO_3^- , and SO_4^{2-} concentrations decreased
354 from the highest ones in 2014 to 9.75 ± 2.89 , 12.29 ± 4.02 , and 30.57 ± 7.43 $\mu\text{eq/L}$ in 2016. The
355 concentrations of Ca^{2+} , NH_4^+ , and Mg^{2+} increased from 31.59 ± 8.29 , 14.84 ± 4.63 , and 8.77 ± 2.42 ,
356 to 58.84 ± 10.31 , 41.33 ± 10.26 , and 10.49 ± 3.07 during 2011-2013 (Fig. 4a), whereas they
357 decreased from the peak values in 2013 to 31.20 ± 8.48 , 18.13 ± 4.84 , and 8.93 ± 2.92 $\mu\text{eq/L}$ in
358 2016, respectively. The F^- concentration exhibited gradual decrease from 3.63 to 2.96 $\mu\text{eq/L}$ during
359 2012-2016. However, the K^+ and Cl^- concentration fluctuated during 2011 and 2016 and did not
360 display regularly annual variation.

361 It was well documented that the SO_4^{2-} concentration was closely associated with the SO_2
362 emissions because SO_2 in the ambient air could be transformed into SO_4^{2-} during aging in the
363 atmosphere (Qiao et al., 2015). In the present study, SO_4^{2-} in the precipitation exhibited a marked
364 correlation with SO_2 in the ambient air ($p < 0.01$), especially with the increased RH (Tab. S2). The
365 total SO_2 emissions in China decreased dramatically due to the installation of the flue gas
366 desulfurization (FGD) systems and the closure of less efficient power plants in China since 2012
367 (Li et al., 2017b). At a national scale, the remarkable decrease of the SO_4^{2-} concentration was
368 observed since 2014, which lagged behind the decrease of the SO_2 emission. Such scenario was



369 widely observed in some developed countries such as Japan (Okuda et al., 2005). However, some
370 cities (i.e., Beijing and Baoding) in NC showed the notable decreases since 2012, which
371 corresponded to the decrease of the total SO₂ emission. It was supposed that the electrostatic
372 precipitators (ESP) and fabric filters (FFs) for the sulfates removal were more widely applied to
373 steel and iron plants, and cement production process, both of which were widely distributed in NC
374 (Hua et al., 2016; Wang et al., 2016b). Moreover, coal has been gradually replaced by natural gas
375 for domestic heating in Beijing, resulting in the less SO₂ emission and thus decreasing the SO₂
376 concentration in the ambient air (Pu et al., 2017). Based on the open data downloaded from National
377 Environmental Monitoring Platform, the annually mean SO₂ concentration in Beijing decreased
378 from 22.0 µg/m³ to 9.29 µg/m³ during 2014-2016, in good agreement with the temporal variation of
379 SO₄²⁻ in the precipitation.

380 The NO_x emission decreased rapidly after the upgrading of oil product quality standards, the
381 import denitrification facilities, and the implementation of low-NO₂ burner technologies (Li et al.,
382 2016; Liu et al., 2017). However, the NO₃⁻ concentration in the precipitation over China only
383 displayed slight decrease during this period. It was assumed that the high NO₃⁻ in the precipitation
384 resulted from the increase of motor vehicles (Link et al., 2017). Based on the bottom-up method,
385 the estimated NO_x emissions from vehicle exhausts in China linearly increased by 75% since 1998
386 (Wu et al., 2016). Shandong suffered from the highest vehicle emissions among all of the provinces,
387 of which the NO_x released from vehicle exhausts in Shandong province increased from 477.6 Gg to
388 513.8 Gg during 2011-2014 (Sun et al., 2016), corresponding to the annual variation of NO₃⁻ in the
389 precipitation of Jinan and Linyi. The NO₃⁻/SO₄²⁻ value was recognized as an important index to
390 determine the relative importance of nitrate (mobile) vs. sulfate (stationary) emission in the



391 atmosphere (Arimoto et al., 1996). The value of $\text{NO}_3^-/\text{SO}_4^{2-}$ at the national scale was still lower than
392 1, suggesting that the contribution of sulfate to the acidity of the precipitation was still higher than
393 that of NO_3^- . Nevertheless, the ratio in the precipitation showed a gradual increase from 0.33 to 0.40
394 during this period, indicating that the precipitation type in China has evolved from sulfuric acid type
395 to a mixed type controlled by sulfuric and nitric acid.

396 The NH_4^+ level in the precipitation was closely linked to the NH_3 emission because NH_3 tended
397 to be neutralized to form $(\text{NH}_4)_2\text{SO}_4$ and NH_4NO_3 in the atmosphere (Zhang et al., 2016). The
398 anthropogenic emission of NH_3 was mainly derived from fertilizer use, livestock manures, vehicle
399 exhausts, and industrial processes (Kang et al., 2016). Wherein, livestock manures and synthetic
400 fertilizer application were considered as two major source of the NH_3 emission, accounting for 80-
401 90% of total emission (Kang et al., 2016; Xu et al., 2016). The nitrogen fertilizer consumption has
402 decreased since 2013 (<http://www.stats.gov.cn/>), which was in good agreement with the variation of
403 the NH_4^+ concentration in the precipitation. Therefore, the fertilizer consumption could be treated
404 as an important factor for the NH_4^+ level in the precipitation. However, the NH_3 emission from
405 livestock manures estimated by Kang et al. (2016) showed an opposite variation to the NH_4^+ level
406 in the precipitation collected herein. It was probably attributed to the slight decrease of air
407 temperature in the major cities of China during 2011-2013 because the actual NH_3 emission to the
408 atmosphere was sensitive to air temperature (Kang et al., 2016), which has been proved by the
409 correlation analysis (Tab. S2). Apart from the contribution source mentioned above, soil served as
410 major natural sources of the NH_3 emissions (Sun et al., 2014). Teng et al. (2017) demonstrated that
411 urban green space made a great contribution to the NH_3 amount in the atmosphere. In the present
412 study, the urban green space in some cities such as Lianyungang (Jiangsu province) and Qingdao



413 (Shandong province) showed the marked correlation with the NH_4^+ level in the wet deposition.

414 The long-range transport of dust aerosol was considered as the major source of Ca^{2+} and Mg^{2+}

415 in the atmosphere (Fu et al., 2014). Song et al. (2016) reported that the magnitude of dust emissions

416 in spring generally decreased in the past decades. The dust deposition and ambient PM_{10}

417 concentration in the Xinjiang autonomous region also decreased dramatically during 2000-2013

418 (Zhang et al., 2017a). Here, Ca^{2+} and Mg^{2+} in the wet deposition of some cities such as Aksu in

419 Xinjiang autonomous region decreased from 32.37 to 4.80 $\mu\text{eq/L}$ and from 15.80 to 4.81 $\mu\text{eq/L}$

420 during 2011-2016, respectively, corresponding to the decrease of dust deposition. However, the

421 decrease of Ca^{2+} and Mg^{2+} over China significantly lagged behind the reduction of dust deposition.

422 It was well known that the increase of soil particles and dusts due to urbanization might induce the

423 high level of Ca^{2+} and Mg^{2+} in the wet deposition (Lyu et al., 2016). The road mileage in China

424 increased by 25% from 2011 to 2013, while it only showed slight increase (2.52%) during 2013-

425 2016 (<http://www.stats.gov.cn/>). Padoan et al. (2017) also demonstrated that the resuspension of

426 road dust generally showed the highest impact on the emission of the Ca and Mg elements among

427 non-exhaust sources (i.e. tire wear, brake wear, road dust).

428 Both of K^+ and Cl^- were identified as the important tracers for biomass burning and fireworks

429 (Cheng et al., 2014). Nevertheless, the K^+ and Cl^- concentration in the precipitation did not reflect

430 the contribution of biomass burning because biomass burning usually occurred in dry seasons (Zhou

431 et al., 2017b). Furthermore, the K^+ concentration in the precipitation showed significantly

432 relationship with crustal ions (Ca^{2+} ($r = 0.40$, $p < 0.01$) and Mg^{2+} ($r = 0.49$, $p < 0.01$)) (Tab. S2),

433 suggesting that other sources could play important role on the accumulation of K^+ and Cl^- . Chen et

434 al. (2017b) recommended that fugitive dust to be the main source of K^+ when the mitigation



435 measures were seriously implemented. The minor F⁻ in the wet deposition served as an indicator of
436 coal combustion because fluorine was generally released from coal combustion (Chen et al., 2013).
437 Recently, the F⁻ emission displayed remarkable decrease because more coal-fired power plants were
438 equipped with FGD and dust removal equipment (Zhao and Luo, 2017), which explained the
439 decrease of F⁻ in the precipitation of some industrial cities such as Baoding (3.22 to 1.65 during
440 2012-2016), Shijiazhuang (3.18 to 2.73), and Handan (3.88 to 3.53) in Hebei province. Na⁺ was
441 generally originated from the transport of sea salt aerosols, fugitive dusts, and the incineration of
442 wastes and fossil fuels (Zhao et al., 2011). The Cl⁻/Na⁺ value in the precipitation of some coastal
443 cities (i.e. Lishui (1.15), Jiaxing (1.20), Dandong (1.18), Wenzhou (1.18)) were similar to the marine
444 equivalent Cl⁻/Na⁺ ratio (1.17) (Wang et al., 2015a), suggesting that Na⁺ in the precipitation of these
445 coastal cities might be derived from ocean. However, the Cl⁻/Na⁺ ratios in the precipitation of some
446 regions far from the ocean were significantly higher than marine equivalent Cl⁻/Na⁺ ratio due to the
447 contribution of coal combustion (Liu et al., 2016b; Liu et al., 2017).

448 3.2.2 The seasonal variation of the inorganic ions in the wet deposition

449 The mean concentrations of SO₄²⁻, NO₃⁻ and F⁻ in the wet deposition were in the order of winter
450 (SO₄²⁻, NO₃⁻ and F⁻: 45.74, 19.44 and 6.10 μeq/L) > spring (42.61, 13.83, and 3.45 μeq/L) > autumn
451 (28.85, 9.73, and 2.67 μeq/L) > summer (19.26, 7.66, and 2.04 μeq/L) (Fig. 4b). It was well known
452 that SO₄²⁻ and NO₃⁻ were usually generated via the oxidation of SO₂ and NO₂ in the atmosphere,
453 respectively (Yang et al., 2016). The combustion of fossil fuels for domestic heating in winter
454 probably promoted the accumulation of SO₂ and NO₂ in the atmosphere (Liu et al., 2017; Lu et al.,
455 2010). Some cities in the NC region including Shijiazhuang and Zhengzhou showed the higher SO₄²⁻
456 and NO₃⁻ levels in the precipitation of winter compared with those in summer, which were in



457 agreement with the seasonal variation of SO_2 and NO_2 concentrations in the ambient air. It reflected
458 that the combustion of fossil fuels for domestic heating contributed to the accumulation of SO_4^{2-} and
459 NO_3^- and these ions deposited via the rainfall. Moreover, stagnant meteorological conditions
460 including shallow mixing layers, high atmospheric pressure, low precipitation, and low wind speed
461 occurred frequently in winter, thereby trapping more pollutants and elevating the concentrations of
462 SO_2 and NO_2 in the atmosphere (Tai et al., 2010). In contrast, strong solar radiation and turbulent
463 eddies from ocean in summer could promote the dispersion of these pollutants (Antony Chen et al.,
464 2001). For instance, some coastal cities such as Beihai (Guangxi autonomous region) and Haikou
465 (Hainan province) were generally exposed of strong solar radiation and high wind speed, which
466 significantly decreased the SO_4^{2-} and NO_3^- concentrations in the precipitation of summer (Beihai:
467 SO_4^{2-} (6.06) and NO_3^- (7.37); Haikou: SO_4^{2-} (5.33) and NO_3^- (4.96)). The F⁻ concentration in the
468 precipitation displayed the similarly seasonal variation to SO_4^{2-} and NO_3^- , which was likely
469 associated with the higher coal consumption for domestic heating in some industrial cities of NC,
470 NWC, and NEC (Ding et al., 2017).

471 The concentrations of Cl^- , Ca^{2+} , K^+ , NH_4^+ , Mg^{2+} , and Na^+ exhibited the highest values in summer,
472 followed by those in spring and autumn, and the lowest one in winter. The higher concentration of
473 NH_4^+ in the precipitation collected in summer was probably linked to agricultural activities. The
474 widespread utilization of fertilizer in summer have been observed over China (Zhang et al., 2011;
475 Tao et al., 2016), which could increase the NH_3 emission. In addition, the NH_3 emission was
476 sensitive to the air temperature and generally increased with the temperature (Kang et al., 2016).
477 The NH_3 released from agricultural activities could transform to NH_4^+ , especially under the
478 condition of high RH (Li et al., 2013). Thus, the high NH_3 emission and rapid photochemical



479 reaction contribute to the higher NH_4^+ in the precipitation in summer. However, K^+ , Ca^{2+} , and Mg^{2+}
480 displayed higher concentrations in spring and summer, which was probably related to the high
481 loading of fugitive dusts (Zhang et al., 2017c). Lyu et al. (2016) demonstrated that the high
482 temperature coupled with strong wind caused the lower water content in the road, leading to higher
483 tendency of dust re-suspension in the Wuhan summer. In the present study, these crustal ions in the
484 precipitation also showed the higher values in the summer of Wuhan. The high concentration of Na^+
485 and Cl^- in spring and summer was probably attributed to the evaporation of sea salt under the
486 condition of high air temperature (Grythe et al., 2014). It was found that Na^+ in summer were 5.1-
487 10.3 times of those in winter in some coastal cities such as Qingdao (5.96) (Shandong province),
488 Qinhuangdao (9.65) (Hebei province), and Sanya (6.83) (Hainan province).

489 3.2.3 Spatial distribution of the water-soluble ions across the whole China

490 At a spatial scale, the annual mean concentrations of NO_3^- , Cl^- , Ca^{2+} , K^+ , F^- , NH_4^+ , Mg^{2+} , SO_4^{2-} ,
491 and Na^+ ranged from 0.20 to 47.98 $\mu\text{eq/L}$, from 0.27 to 80.86 $\mu\text{eq/L}$, from 0.59 to 157.15 $\mu\text{eq/L}$,
492 from 0.15 to 23.43 $\mu\text{eq/L}$, from 0.11 to 11.64 $\mu\text{eq/L}$, from 0.20 to 84.24 $\mu\text{eq/L}$, from 0.28 to 39.30
493 $\mu\text{eq/L}$, from 0.29 to 191.95 $\mu\text{eq/L}$, and from 0.15 to 39.50 $\mu\text{eq/L}$ during 2011-2016, respectively.
494 All of these water-soluble ions displayed significantly spatial variation, as shown in Fig. 5 and Fig.
495 6.

496 The mean concentrations of the secondary ions (NO_3^- , NH_4^+ , and SO_4^{2-}) showed the highest
497 values in YRD (Changzhou (34.53, 73.40, and 80.47 $\mu\text{eq/L}$) (Fig. 5a-c) and Nanjing (35.62, 17.12,
498 and 49.51 $\mu\text{eq/L}$) and SB (Chengdu (38.08, 65.19, and 57.16 $\mu\text{eq/L}$) and Leshan (25.32, 38.99, and
499 61.24 $\mu\text{eq/L}$)), followed by ones in NC (Jinan (11.67, 16.57, and 58.28 $\mu\text{eq/L}$) and Anyang (20.46,
500 41.32, and 22.01 $\mu\text{eq/L}$), and the lowest ones in TB (0.50, 0.91, and 1.44 $\mu\text{eq/L}$) (Lhasa). Many



501 secondary ions exhibited the high concentrations in YRD because of intensive energy consumption
502 and industrial activities (Zhou et al., 2017a). For instance, the total energy consumption of the
503 Jiangsu province was second to Hebei province among all of the provinces in China (Wang 2014).
504 The SO₂ and NO_x emissions from cement plants and iron and steel industries in Jiangsu and Zhejiang
505 province were significantly higher than those in other provinces (Hua et al., 2016; Wang et al.,
506 2016b), which was in coincident to the spatial agglomeration of the SO₂ and NO₂ concentrations in
507 the ambient air of these provinces It has been reported that the acid deposition pattern have moved
508 from SWC to SEC since 2000s (Yu et al., 2017a). However, SB still possessed high concentrations
509 of secondary ions in the precipitation because of high S content in the local consumed coals (Ren et
510 al., 2006). Besides, the unique topographic conditions and unfavorable diffusion conditions
511 facilitated the deposition of regionally transported pollutants stuck by Qinling mountains and Daba
512 mountain (Kuang et al., 2016), although the energy consumption of Sichuan province was much
513 less than those in other provinces (Tian et al., 2013). Moreover, the steady increase use of fertilizer
514 and livestock manures coupled with high air temperature made SB to be one of the NH₃ emission
515 hotspots (Li et al., 2017a). Nevertheless, some remote areas in NWC and SWC such as Lhasa and
516 Aba showed the lower secondary ions due to sparse population and anthropogenic activities (Li et
517 al., 2007). In these regions, these secondary ions were mainly derived from crustal source, and then
518 deposited concurrently in the rainfall events (Niu et al., 2014). Besides, relatively extensive
519 anthropogenic activities such as increased vehicle exhaust might promote the emissions of
520 secondary ions in the tourist season (Qiao et al., 2017). For instance, the number of tourists in Lhasa
521 have been increasing to 11 million until 2015 ([http://www.xinhuanet.com/fortune/2016-](http://www.xinhuanet.com/fortune/2016-01/13/c_1117763885.htm)
522 [01/13/c_1117763885.htm](http://www.xinhuanet.com/fortune/2016-01/13/c_1117763885.htm)), which could boost the slight increase of secondary ions in the wet



523 deposition.

524 F⁻ showed the higher concentrations in NC, YRD, and SB because many coal-fired power plants
525 and iron and steel industries were mainly concentrated in the Hebei and Jiangsu province (Liu et al.,
526 2015a) (Fig. 6a). Besides, Hebei and Jiangsu were two provinces with much higher coal
527 consumptions (Li et al., 2017), which could release large quantity of F⁻ to the atmosphere. Although
528 the power plants and iron and steel industries were relatively scarce in SB, many large phosphorite
529 mines might increase the F⁻ concentration in the precipitation (Wu et al., 2014). As one of the largest
530 phosphorite mine over China, Jinhe phosphorite mine was close to Chengdu, which significantly
531 increased the F⁻ concentration in the precipitation of Chengdu (9.21 µeq/L). Moreover, the high
532 abundance of F⁻ in the local coal (Mianyang: 269.25 µg/g, Guangan: 1061 µg/g) also contributed to
533 the F⁻ emissions (Dai and Ren, 2006; Wang et al., 2016c; Ren et al., 2006). In addition, the F⁻ in the
534 precipitation showed remarkable relevance with T_{max} based on the correlation analysis ($r = 0.12$, p
535 < 0.05). The annually mean air temperature in SB (17.2 °C) were slightly higher than that in Hebei
536 (14.3 °C) and Jiangsu (16.4 °C) province, thereby boosting the F⁻ emission.

537 The high concentrations of Cl⁻ were mainly concentrated on coastal cities such as Shanghai,
538 Lianyungang (Jiangsu province) and Qingdao (Shandong province) (Fig. 6b), indicating the effect
539 of sea-salt sourced from the ocean (Gu et al., 2011; Allen et al., 2015; Grythe et al., 2014). The high
540 Na⁺ concentration not only focused on these coastal cities (Fig. 6c), but also enrich in some arid and
541 semi-arid cities such as Jinchang (35.08 µeq/L) and Gannan (25.51 µeq/L) (Gansu province). It was
542 assumed that the windblown dust originated from Taklimakan Desert could play a vital role on the
543 enrichment of Na⁺ in Inner Mongolia and Hexi corridor because these regions were located on the
544 downwind direction of dust (Engelbrecht et al., 2016). Meanwhile, the evaporation of salt lakes in



545 West China might promote the Na^+ enrichment in the precipitation (Bian et al., 2017). Besides, the
546 dust event also promoted the elevation of Ca^{2+} , especially in Jiayuguan and Guyuan (Gansu province)
547 (Fig. 6d), both of which were located in the Hexi corridor (Allen et al., 2015). The Mg^{2+} presented
548 higher value in some cities (Handan: 36.63 $\mu\text{eq/L}$, Liupanshui: 39.30 $\mu\text{eq/L}$) in the Hebei province
549 and Guizhou province (Fig. 6e). The soil in the Guizhou province possessed the highest Mg
550 concentration (843.33 mg/kg) in China (Li et al., 1992), where the Mg^{2+} stored into the soils could
551 be lifted into the atmosphere by strong wind coupled with severe stony desertification (Jiang et al.,
552 2014). Although the Mg concentration in the soil of Hebei province was slightly lower compared
553 with those of Guizhou province, the bioavailable Mg concentration peaked in Hebei province (Hao
554 et al., 2016), which could be inclined to re-suspend into the atmosphere and then deposit with the
555 rainfall in the warm season.

556 3.2.4 Neutralization capacity of the alkaline ions

557 In order to reveal the most important ion for neutralization (Ca^{2+} , NH_4^+ , and Mg^{2+}) in the
558 precipitation, the relative proportion of three NFs in all of the cities are summarized in Fig. 7. The
559 triangular diagram showed that the contribution of three ions were in the order of Ca^{2+} (51.84%) >
560 NH_4^+ (34.14%) > Mg^{2+} (14.02%). The NF ratios of NH_4^+ and Ca^{2+} in China displayed the highest
561 values in summer, followed by ones in spring and autumn, and the lowest one in winter (Fig. 7a). It
562 was supposed that strong acid neutralization were mainly brought about by the alkaline ions via
563 high rainfall. Besides, the neutralization capacity of the alkaline ions reached higher in spring due
564 to the effects of dust events (Wang et al., 2015b). In the present study, the NFs of NH_4^+ and Ca^{2+} in
565 Beijing (NH_4^+ : 0.57, Ca^{2+} : 0.17) and Baoding (NH_4^+ : 0.56, Ca^{2+} : 0.19) showed the markedly higher
566 values in spring. Zhai and Li (2003) also observed that most frequent dust storms generally occurred



567 in NC in spring. However, the NFs of Mg^{2+} (0.70) showed the highest one in winter. Aside from the
568 temporal difference of neutralization, the NFs presented a significantly spatial variation in China
569 (Fig. 7b). The high NFs of Ca^{2+} were mainly concentrated on some cities in NWC such as
570 Bayingolin (0.57) because these arid and semi-arid regions were exposed of periodic Asian dust
571 intrusions (Yu et al., 2017b). In the case of the typical dust events, the content of crustal species
572 such as Ca increased substantially (Chen et al., 2015). Compared with the other regions, the NFs of
573 NH_4^+ showed the higher value in some cities of SWC such as Chengdu (0.55). Kang et al. (2016)
574 demonstrated that the NH_3 emissions in Sichuan province were significantly higher than those in
575 other provinces of China, accounting for more than 10 % of the total emission from livestock
576 manures. The NFs of Mg^{2+} peaked in NC, which was in good agreement with the higher
577 concentration of Mg^{2+} in the wet deposition of NC. The higher concentration of bioavailable Mg^{2+}
578 in the soil was beneficial to increase the neutralization capacity of Mg^{2+} in the wet deposition (Hao
579 et al., 2016), although the SO_2 and NO_2 emissions in NC were significantly higher than those in
580 other regions (Fu et al., 2016).

581 3.3 Comparisons of pH, EC, and the inorganic ion concentrations with the previous studies

582 The annual mean pH, EC and the inorganic ion levels in the precipitation of some metropolitans
583 across China are summarized in Tab. 1. The mean pH values of the most cities in SEC and SWC
584 (i.e., Shanghai: 4.39 and Wuhan: 4.68) were lower than those in some remote areas such as
585 Jiuzhaigou (5.95) and Yulong mountain (5.94) (Qiao et al., 2018; Niu et al., 2014), while the average
586 pH values of some cities in NC and NWC such as Zhengzhou (6.09) and Urumqi (6.13) were slightly
587 higher than those in remote areas. It was assumed that the remote areas were less affected
588 anthropogenic source except local tourist activities, while high aerosol emissions were mainly



589 centered on some metropolitans of SEC and SWC. The pH of the precipitation in Zhengzhou (pH =
590 6.09) (Henan province) and Urumqi (pH = 6.13) (Xinjiang autonomous region) showed high value
591 compared with some remote regions because of the strong neutralization capacity of alkaline ions
592 (Wang et al., 2014). Besides, the pH values in the wet deposition of most metropolitans in China
593 were also lower than those in some developing countries (e.g., Guaiba: 5.92, Petra: 6.80) (Tab. 1).
594 It was supposed that SO₂ and NO_x emitted from industrial and vehicle emissions in China could be
595 higher than those in some countries such as Brazil and Jordan (Wu and Han 2015). In addition,
596 higher abundance of the neutralizing components in Jordan tended to increase pH of the
597 precipitation. On the other hand, the pH values of the wet deposition in most cities of China were
598 significantly higher than those in some cities of developed countries such as Sardinia (pH = 5.18)
599 (Italy) and Adirondack (pH = 4.50) (United States). It was assumed that many Western countries
600 were faced up with severe acid issue due to the rapid industrialization before 2002 (Sickles II and
601 Shadwick 2015). In addition, the annually mean rainfall amount in some cities of East China were
602 higher than those in Sardinia and Adirondack, which could dilute the acidity of the precipitation
603 (Tsai et al., 2011). The mean EC in the wet deposition of most cities over China were approximate
604 to those in some remote regions (i.e., Yulong Mountain, Jiuzhaigou), and some foreign cities such
605 as Guaiba, Brazil. However, Lanzhou (EC = 58.06 μS cm⁻¹) (Gansu province) and Petra (EC = 160
606 μS cm⁻¹) (Jordan) showed remarkably higher value than other cities, suggesting that the dust
607 cyclones from Taklamakan and Khamaseen played vital roles on the EC and chemical composition
608 in the precipitation (Abed et al., 2009).

609 The concentrations of NO₃⁻, SO₄²⁻, and NH₄⁺ in the most cities of China except Qingdao
610 (Shandong province) and Lhasa (Tibet autonomous region) were significantly higher than those in



611 some natural reserve areas such as Jiuzhaigou, Yulong Mountain, and Nam Co (Qiao et al., 2018;
612 Niu et al., 2014) (Tab. 1), suggesting the local point and non-point emissions in these cities played
613 important roles on the concentrations of inorganic ions in the precipitation. However, the
614 concentrations of these inorganic ions in the most cities were lower than those in foreign cities such
615 as Singapore, Petra (Jordan), Tokyo, and Newark (United States) (Balasubramanian et al., 2001; Al-
616 Khashman et al., 2005; Okuda et al., 2005; Song and Gao 2009), indicating the effects of restricting
617 emissions of air pollutants since Chinese 12th Five-Year Plan (Liu et al., 2016a). However, some
618 cities including Shenyang (Liaoning province) and Chengdu (Sichuan province) were still faced up
619 with severe acid deposition. On the whole, the concentrations of the crustal ions (Ca^{2+} and Mg^{2+})
620 were in the order of the arid and semi-arid cities/regions (Nam Co, Urumqi, Lanzhou, and Petra) >
621 the inland cities and natural reserve regions (Chengdu and Yulong mountain) > the coastal cities
622 (i.e., Guaiba, Singapore, and Tokyo). Kang et al. (2016) reported that Tibetan Plateau have been
623 frequently affected by dust events under the condition of climate change in the past decades, which
624 probably increased the Ca^{2+} and Mg^{2+} levels in Nam Co. However, it should be noted that some
625 coastal cities such as Patras (Greece) and Sardinia (Italy) possessed higher Ca^{2+} and Mg^{2+} levels,
626 which was probably attributed to the long transport of the dust from of the Sahara desert (Kabatas
627 et al. 2014). Cabello et al. (2016) demonstrated that African air masses mostly reached some coastal
628 cities of Mediterranean on the basis of back-trajectory analysis.

629 3.4 The source apportionment of the ions in the precipitation across China

630 3.4.1 EF and geochemical index method

631 The mean values of EFs (seawater and soil), SSF and CF in all of the cities are listed in Tab. 2.

632 The water-soluble ion was treated to be enriched relative to the reference source when the EF value



633 of the ion was significantly higher than 1.00, whereas it was considered to be diluted when the EF
634 value of the ion was not much higher than 1.00. In the present study, the mean EF_{sea} for Na^+ , Cl^- ,
635 SO_4^{2-} , NH_4^+ , K^+ , Mg^{2+} , Ca^{2+} , NO_3^- , and F^- over China were 1.00, 1.13, 7.22, 10.51, 16.16, 18.18,
636 231.56, 3507.49, and 5864.28, suggesting that Cl^- and Na^+ in the precipitation were enriched in the
637 marine origin at a national scale. The mean EF_{soil} of Mg^{2+} , K^+ , Ca^{2+} , Na^+ , SO_4^{2-} , F^- , NO_3^- , NH_4^+ , and
638 Cl^- reached 0.55, 0.83, 1.00, 1.83, 5.13, 9.96, 59.36, 86.31, and 169.88, indicating that Ca^{2+} , K^+ , and
639 Mg^{2+} were considered to be originated from the crustal source. Both of the EF_{sea} for SO_4^{2-} and NO_3^-
640 showed significantly spatial variability and they presented the higher ones in YRD and SB
641 (significantly higher than 1) (Fig. 8a-b), which suggested that both of the ions were not mainly
642 sourced from the sea source. However, EF_{sea} for SO_4^{2-} in some cities such as Nujiang (0.92) and
643 Nanchong (0.81) were lower than 1. It was assumed that the Indian monsoon played an important
644 role on the wet deposition of SO_4^{2-} (Gu et al., 2016). Except SO_4^{2-} and NO_3^- , EF_{sea} for other ions
645 showed relatively uniform distribution at a national scale. EF_{sea} for NH_4^+ , F^- , Ca^{2+} , K^+ , and Mg^{2+} in
646 most of the cities were higher than 1 (Fig. 8c and S1), indicating the effects of anthropogenic source
647 or crustal source. The EF_{sea} for Cl^- presented the lower value in many coastal cities such as Beihai
648 (0.53) and Haikou (0.52), while they were significantly higher than 1 in some inland cities such as
649 Daqing (13.11). The spatial variability of EF_{sea} for Cl^- confirmed the spatial difference of Cl^-/Na^+
650 between coastal cities and inland ones mentioned above. Compared with EF_{sea} , the EF_{soil} of ions
651 generally displayed remarkably spatial variation. The EF_{soil} of SO_4^{2-} , NO_3^- , F^- , and Cl^- showed
652 notably higher values in SEC, implicating the effects of industrial activity (Fig. 8a-b and S2a-b).
653 The EF_{soil} of NH_4^+ presented markedly higher value in the eastern region of Inner Mongolia and
654 Heilongjiang province such as Hegang (325.69) (Fig. 8c) because intensive grazing was beneficial



655 to the NH_3 emission (Kobbing et al., 2014). It was interesting to note that the EF_{soil} of Na^+ showed
656 higher value in some cities around Qinghai Lake and the evaporation of salt lake could contribute
657 to the higher EF_{soil} of Na^+ (Fig. S2c). The EF_{soil} of crustal ions such as Mg^{2+} and K^+ in NWC were
658 close to 1, reflecting the contributions of dust events and soils (Fig. S2e-f).

659 Based on the EF_{sea} and EF_{soil} , the estimated SSF, CF, and AF of ions are depicted in Fig. 9, S3,
660 and S4. The mean SSF values of NO_3^- , F^- , Ca^{2+} , NH_4^+ , Mg^{2+} , K^+ , SO_4^{2-} , Cl^- , and Na^+ were 0%,
661 0.02%, 0.06%, 0.10%, 2.94%, 4.88%, 13.85%, 88.31%, and 100%, respectively. The average CF
662 values of NH_4^+ , NO_3^- , Cl^- , F^- , SO_4^{2-} , Na^+ , K^+ , Mg^{2+} , and Ca^{2+} reached 0.01%, 0.02%, 0.59%, 10.04%,
663 19.50%, 35.34%, 95.12%, 97.06%, and 99.94%, respectively. The AF value was considered to be
664 the contribution ratio of each ion except SSF and CF. The AF values of Ca^{2+} , K^+ , Mg^{2+} , Na^+ , Cl^- ,
665 SO_4^{2-} , F^- , NH_4^+ , and NO_3^- reached 0%, 0%, 0%, 0%, 11.10%, 66.65%, 89.94%, 99.89%, and 99.98%,
666 respectively. The results suggested that NO_3^- , SO_4^{2-} , NH_4^+ , and F^- were mainly sourced from
667 anthropogenic activities based on minor SSF and CF. It was well documented that the combustion
668 of fossil fuels, iron and steel industrial emission, and vehicle exhaust were main sources of SO_4^{2-}
669 and NO_3^- across China (Song et al., 2006; Yang et al., 2016). In the present study, the AF values of
670 NO_3^- in all of cities were higher than 90%, and those of SO_4^{2-} in half of the cities were higher than
671 60%. Besides, the utility of nitrogen fertilization, and human and livestock excretions were treated
672 as the main source of NH_4^+ emission over China (Cao et al., 2009). Herein, 82.5% of cities across
673 China showed the higher AF value of NH_4^+ (> 90%). Ca^{2+} , K^+ , and Mg^{2+} were mainly derived from
674 crustal origin based on the high CF values. Although the K^+ concentration in the fine particles was
675 usually sourced from biomass burning, the component in the coarse particles generally resulted from
676 the soil erosion and dust re-suspension (Cao et al., 2009). The higher CF values of K^+ in most of



677 cities in China such as Aksu (Xinjiang autonomous region) and Bayin (Gansu province) suggested
678 that the wet deposition has become the main removal mechanism for the K^+ in the coarse particles
679 (Lim et al., 1991). The Na^+ and Cl^- ions were mainly originated from sea source because they were
680 main components of sea-salt and sea-spray aerosol (Prather et al., 2013), which was also supported
681 by the higher SSF value.

682 At a spatial scale, the highest AF values of NO_3^- , SO_4^{2-} , NH_4^+ , and F were mainly concentrated
683 on East China and SWC (Fig. 9a-c, S3a-c), which was similar to the spatial variation of population.
684 The emissions of aerosols and their precursors released by human activities were mainly
685 concentrated on East China (Fu and Chen 2016), thereby leading to high AF values of these
686 secondary ions. Indeed, many cities in NC such as Handan and Shijiazhuang showed the higher AF
687 value, which revealed the effects of power plant, non-ferrous smelting, and coal mining. The SSF
688 value of Cl^- exhibited high value in Xinjiang and Qinghai province (i.e., Altay and Haibei), SWC
689 (i.e., Chengdu and Guangan) (Fig. S3d-e), and some coastal cities (i.e., Ningbo and Shanghai). The
690 higher SSF values of Cl^- in SWC and coastal cities of East China were mainly controlled by Indian
691 monsoon and East Asia monsoon driven atmospheric transport, respectively (Gu et al., 2016).
692 However, it was assumed that the higher SSF value of Cl^- in the region close to Qinghai Lake could
693 be linked to the evaporation of saline (Bian et al., 2017). However, the relatively higher CF value
694 of Cl^- was centered on Ningxia autonomous region and Shaanxi province, which was frequently
695 exposed of Aeolian dust especially under the process of wind erosion (Lyu et al., 2017). As the
696 typical crustal ions, K^+ and Mg^{2+} in the most regions of China generally showed high CF values,
697 especially in some cities of SWC (i.e., Guiyang, Zunyi, Zhaotong) (Fig. S4a-d). It was supposed
698 that the severe soil erosion and loss, and rocky desertification frequently observed in Yungui Plateau



699 contributed to the higher CF value in this region (Jiang et al., 2014). The SSF of K^+ and Mg^{2+}
700 showed high values in some coastal cities (i.e., Sanya and Ningbo), and some cities of NWC such
701 as Haibei (Qinghai). The evaporation of salt in East China Sea and Qinghai Lake could play a vital
702 role on the K^+ and Mg^{2+} in these areas (Bian et al., 2017).

703 3.4.2 The FA-MLR analysis

704 In order to enhance the reliability of source identification, the FA method was also utilized to
705 identify the source of chemical compositions in the precipitation. The FA results of four seasons are
706 summarized in Tab. 3. Three principal components were extracted from the rainwater samples, all
707 of which explained 85.6% of the total variance. The Kaiser-Meyer-Olkin indicator (0.85) was higher
708 than 0.7, suggesting that three factors extracted in the present study was reasonable. Factor 1
709 grouped NO_3^- , F, NH_4^+ , and SO_4^{2-} , accounting for 52.3% of the variance, which was generally
710 associated with dense anthropogenic activities (Nayebare et al., 2016; Zhang et al., 2017b). Factor
711 2 displayed high loadings of Na^+ and Cl^- , indicating the effects of sea-salt and sea-spray aerosol
712 (Gupta et al., 2015). The result was also in good agreement with the high SSF value of Na^+ and Cl^-
713 supported by geochemical index method. Factor 3 occupied 9.54% of the total variance and was
714 dominated by Ca^{2+} , Mg^{2+} , and K^+ . The former two ions were considered to be the important
715 indicators of crustal origin or windblown dust source, which were commonly stored in soils and
716 dusts (Kchih et al., 2015). K^+ was also observed in urban fugitive dusts, although it was generally
717 considered as an important fingerprint of biomass burning (Shen et al., 2016). As a whole, the result
718 of FA was in coincident with that obtained from the EF and geochemical index method.

719 Although the key origins were isolated via the FA method, the contribution ratio of these
720 sources to the water-soluble ions were still unknown. Thus, the FA-MLR method was further applied



721 to quantify the contribution ratio of several sources to these ions in the 320 cities over China (Fig.
722 10a-d). In four seasons, the mean contributions of the anthropogenic source (NO_3^- , SO_4^{2-} , NH_4^+ , and
723 F^- : 79.10%, 46.12%, 82.40%, and 71.02%) were significantly higher than those of sea source
724 (13.76%, 31.71%, 11.09%, and 11.52%) and crustal origin (7.14%, 22.17%, 6.52%, and 17.46%)
725 for NO_3^- , SO_4^{2-} , NH_4^+ , and F^- . Nevertheless, the contribution ratio was in the order of crustal origin
726 (K^+ , Ca^{2+} , and Mg^{2+} : 77.44%, 82.17%, and 70.51%) > anthropogenic source (13.91%, 10.20%, and
727 18.36%) > sea source (8.65%, 7.64%, and 11.14%) for K^+ , Ca^{2+} , and Mg^{2+} . The sea source was the
728 dominant factor for the accumulation of Na^+ and Cl^- in the rainwater, followed by the crustal origin
729 and the anthropogenic source. In addition, the contribution ratios of three sources showed the slight
730 variation in different seasons (Fig. 10). For instance, the contribution ratio of sea source to most
731 inorganic ions especially Na^+ and Cl^- displayed the highest one in summer, followed by ones in
732 spring and autumn, and the lowest one in winter because the intense evaporation of sea salt in
733 summer was inclined to release more ions to the atmosphere (Teinilä et al., 2014). The contribution
734 ratio of anthropogenic activities presented the notable increase from summer to winter for SO_4^{2-}
735 because of dense coal combustion (20 kg coal/m²) for domestic heating in winter (Zhao et al., 2016).

736 3.5 The deposition flux of the water-soluble ions and their key factors

737 At a national scale, the annually mean deposition fluxes of NO_3^- , Cl^- , Ca^{2+} , K^+ , F^- , NH_4^+ , Mg^{2+} ,
738 SO_4^{2-} , and Na^+ over China were 13.25, 8.44, 13.80, 2.49, 1.15, 5.90, 2.27, 33.41, and 4.39 kg ha⁻¹
739 yr⁻¹ during 2011-2016. The deposition fluxes of NO_3^- , Ca^{2+} , K^+ , NH_4^+ , and Na^+ increased from 13.67
740 to 14.83 kg ha⁻¹ yr⁻¹, 13.32 to 16.99 kg ha⁻¹ yr⁻¹, 2.47 to 2.79 kg ha⁻¹ yr⁻¹, 5.21 to 6.48 kg ha⁻¹ yr⁻¹,
741 and 4.17 to 5.74 kg ha⁻¹ yr⁻¹ from 2011 to 2013, respectively. However, they increased to 13.65,
742 11.01, 2.52, 5.90, and 3.69 kg ha⁻¹ yr⁻¹ in 2016. The wet deposition fluxes of F^- and Mg^{2+} over China



743 decreased from 1.27 to 0.96 kg ha⁻¹ yr⁻¹ and 2.76 to 1.85 kg ha⁻¹ yr⁻¹ during 2012-2014, respectively.
744 However, they began to increase slightly to 1.17 and 2.15 in 2016, respectively. The wet deposition
745 fluxes of Cl⁻ and SO₄²⁻ showed gradual decrease from 9.80 and 38.87 kg ha⁻¹ yr⁻¹ to 8.09 and 26.54
746 kg ha⁻¹ yr⁻¹ during 2011-2016, respectively. On average, the wet deposition flux of NO₃⁻ were higher
747 by 2.25 times than that of NH₄⁺, which was in contrast to the results of the dry deposition reported
748 by Xu et al. (2015). All of the water-soluble ions showed the highest wet deposition fluxes in
749 summer, followed by ones in spring and autumn, and the lowest ones in winter, which was probably
750 attributed by the high washout effect due to rain in summer (Jia et al., 2014). Based on the results
751 of the correlation analysis, the precipitation showed the significant relationship with the deposition
752 fluxes of the water-soluble ions ($p < 0.05$). In addition, the wet deposition fluxes of the water-soluble
753 ions showed the significantly spatial variation, which were in good agreement with the spatial
754 distribution of the water-soluble ion concentrations except Ca²⁺ (Fig. S5).

755 In order to determine the dominant factors affecting the wet deposition fluxes of the water-
756 soluble ions across China, GDP, GIP, TEC, N fertilizer use, vehicle ownership, UGS, dust days,
757 many meteorological factors (i.e., T_{max}, T_{min}, WS), and air pollutants (i.e., SO₂ and NO₂) were
758 introduced as the explanatory variables. The SR analysis results are depicted in Tab. 4. GIP, vehicle
759 ownership, NO₂, T_{min}, and wind speed served as the key factors affecting apparently the wet
760 deposition of NO₃⁻ at a national scale. The atmospheric emission of NO_x from coal-fired power
761 plants was estimated about 7489.6 kt in 2010, although many newly built power plants were
762 equipped with advanced low NO_x burner (LNB) systems (Tian et al., 2013). Zhang et al. (2014)
763 estimated that NO_x from vehicle emissions reached 4570 kt in 2008, which was considered as the
764 second NO_x source only to industrial activities. The NO_x released from anthropogenic activity could



765 enhance the NO_2 concentration in the ambient air, which could be also transformed to NO_3^- via
766 oxidation in the atmosphere, especially under the condition of high temperature and low WS (Zhang
767 et al., 2016). The wet deposition of NH_4^+ were affected by N fertilizer use, UGS, and NO_2 over
768 China. Russel et al. (1998) recommended early that NH_4^+ in the precipitation was most likely
769 derived from the N fertilizer use via an isotope techniques coupled with back trajectory analysis.
770 Besides, Teng et al. (2017) demonstrated that the emission from UGS was identified to contribute
771 to the atmospheric NH_3 significantly during 60% of the sampling times, which could increase the
772 NH_4^+ concentration in the precipitation due to the photochemical reaction. The wet deposition flux
773 of SO_4^{2-} was closely associated with TEC in the 320 cities of China, respectively. It was supposed
774 that the SO_2 emission were dependent on the use of coal and petroleum (Lu et al., 2010). While
775 terrestrial petroleum emissions have declined in recent years, the emissions from international
776 shipping have offset the decrease of terrestrial petroleum (Smith et al., 2011). In the present study,
777 the deposition of some crustal ions were linked to the dust days because they were mainly derived
778 from the dust storm or soil (Deshmukh et al., 2011; Zhang et al., 2011). The F deposition was
779 associated with GIP due to the contributions of the coal-fired power plant fly ash and industrial raw
780 material (Kong et al., 2011).

781 The GWR method was used to calculate the local regression coefficients in order to determine
782 the dominant factor affecting the deposition of the water-soluble ions at the regional scale (Fig. 11
783 and S6). The mean R^2 of GWR method was 0.50 over China, and the p value was lower than 0.05,
784 which suggested that the GWR method could be applicable to the study. The local regression
785 coefficient of dust days for crustal ions including Ca^{2+} , Cl^- , K^+ , and Mg^{2+} increased from SEC to
786 NWC (Fig. S6a-e), suggesting that dust days played a significant role on the crustal ions in NWC



787 due to high intensity of dust deposition and extremely high WS (Zhang et al., 2017a). The influence
788 of GIP on the F^- and NO_3^- increased from West China to East China, and displayed the higher value
789 in some cities of YRD (i.e., Shanghai, Hangzhou) because many coal-fired power plants, cement
790 plants, and municipal solid waste incineration plants were located in YRD (Hua et al., 2016; Tian et
791 al., 2012; Tian et al., 2014) (Fig. S6f and 11a). The influence of N fertilizer use on NH_4^+ was
792 concentrated on some cities of NEC such as Jiamusi (Heilongjiang province) (Fig. 11b-c), Harbin
793 (Heilongjiang province), Changchun (Jilin province) because the largest commodity grain base were
794 located in Heilongjiang and Jilin province, leading to the higher N fertilizer use (Cheng and Zhang,
795 2005). In contrast to the effects of GIP, the TEC influence increased gradually from SEC to NWC,
796 and showed the highest value in Xinjiang autonomous region (i.e., Altay) (Fig. 11d). It has been
797 demonstrated that an inverted U-shaped curve (Environment Kuznets Curve) between per capita
798 GDP and energy consumption was generally observed during the development of economy (Song
799 et al., 2013; Yang et al., 2017). The Environment Kuznets Curve denoted that the energy
800 consumption displayed positive relationship with per capita GDP in the early stage of development.
801 However, the positive relationship tended to transform into the negative relevance with the
802 development of economy because the reliance on the energy-intensive industries would be reduced
803 in the developed stage (Yang et al., 2017). It was assumed that Xinjiang autonomous region kept at
804 the early stage of the inverted-U curve and largely rested on the energy-intensive industries as the
805 less-developed province (Yang et al., 2017). However, some developed provinces in SEC such as
806 Zhejiang and Jiangsu have sped up structural transformation of the economy and reduce the reliance
807 on the heavy industries. The influence of UGS and vehicle ownership peaked in Shandong province
808 (i.e., Qingdao, Jinan) and YRD (i.e., Shanghai, Hangzhou) (Fig. 11e-f). It was supposed that the



809 UGS and vehicle ownership in these cities showed higher values among all of the 320 cities
810 (National Bureau of Statistics of China). Apart from the effects of socioeconomic factors, the
811 meteorological factors also played significant roles on NO_3^- . The influences of air temperature and
812 WS both increased from East China to West China, and showed the highest values in Xinjiang
813 province (Fig. 11g-h). Zhang et al. (2017a) demonstrated that the strong dust events along with high
814 WS contributed to the neutralization of NO_3^- , although the NO_2 concentrations in some cities of
815 Xinjiang province were significantly higher than other regions of China.

816 4. Conclusions

817 This study newly reported spatiotemporal variation of nine water-soluble ions in the
818 precipitation across the whole China during 2011-2016. The mean pH and EC values varied
819 significantly compared with those during 1980-2000 because the implementation of special air
820 pollution control measures have mitigated the air pollution in China. The concentrations of Na^+ ,
821 NO_3^- , and SO_4^{2-} increased from 7.26 ± 2.51 , 11.56 ± 3.71 , and 33.73 ± 7.59 $\mu\text{eq/L}$ to 11.04 ± 4.64 ,
822 13.59 ± 2.63 , and 41.95 ± 8.64 $\mu\text{eq/L}$ during 2011 and 2014, while they decreased from the highest
823 ones in 2014 to 9.75 ± 2.89 , 12.29 ± 4.02 , and 30.57 ± 7.43 $\mu\text{eq/L}$ in 2016, respectively. The
824 concentrations of Ca^{2+} , NH_4^+ , and Mg^{2+} increased by 86.26%, 178.50%, and 19.71% from 2011 to
825 2013, whereas they decreased from 58.84 ± 10.31 , 41.33 ± 10.26 , and 10.49 ± 3.07 in 2013 to 31.20
826 ± 8.48 , 18.13 ± 4.84 , and 8.93 ± 2.92 $\mu\text{eq/L}$ in 2016, respectively. The concentration of F^- decreased
827 linearly by 5.58%/yr during 2012-2016. The mean concentrations of SO_4^{2-} , NO_3^- and F^- showed the
828 highest values in winter, followed by ones in spring and autumn, and the lowest ones in summer. It
829 was supposed that the dense anthropogenic activities such as domestic combustion for heating and
830 adverse meteorological conditions. The crustal ions (Ca^{2+} , Mg^{2+} , and K^+) peaked in spring and



831 summer, suggesting the contributions of fugitive dusts. The Na^+ and Cl^- were markedly affected by
832 evaporation of sea salt. All of the water-soluble ions in the precipitation exhibited notably spatial
833 variability. The secondary ions (SO_4^{2-} , NO_3^- and NH_4^+), and F^- peaked in YRD (i.e., Changzhou,
834 Hangzhou, and Nanjing) owing to the intensive energy consumption and industrial activities. The
835 higher S content in the coal and unfavorable diffusion conditions contributed to the higher
836 concentrations of secondary ions in SB (i.e., Chengdu, Leshan, and Dazhou). The crustal ions and
837 sea-salt ions showed the highest concentrations in semi-arid regions (i.e., Guyuan, Jiayuguan) and
838 coastal cities (i.e., Qingdao, Lianyungang), respectively.

839 The EF method, geochemical index method, and FA-MLR method consistently suggested that
840 NO_3^- , F^- , NH_4^+ , and SO_4^{2-} were dominated by anthropogenic activities. However, the Na^+ and Cl^-
841 were closely associated with sea-salt aerosol. Ca^{2+} , Mg^{2+} , and K^+ were mostly derived from crustal
842 source. The SR analysis and GWR method implied that GIP, TEC, vehicle ownership, and N
843 fertilizer use played the important roles on SO_4^{2-} , NO_3^- , NH_4^+ , and F^- . However, the crustal ions
844 were significantly affected by dust events. The correlation between influential factors and the ions
845 in the wet deposition showed significantly spatial variability. The influence of dust days on the
846 crustal ions increased from SEC to NWC, whereas the influence of socioeconomic factors on
847 secondary ions showed the highest value in East China.

848 The present study validate the model estimations of the water-soluble ions deposition at a
849 national scale, and provide the fundamental data for the prevention and control of acid deposition
850 and air pollution. However, there were several plausible contributors to the uncertainty. First of all,
851 the monitoring sites were distributed unevenly and relatively scarce sites were located in Northwest
852 China. Moreover, the limited independent variables were included into the models. Thus, further



853 studies were required to establish more representative monitoring sites and incorporate more
854 variables to reduce the uncertainty associated with the ions deposition.

855 **Acknowledgements**

856 This work was supported by National Key R&D Program of China (2016YFC0202700), National
857 Natural Science Foundation of China (Nos. 91744205, 21777025, 21577022, 21177026),
858 International cooperation project of Shanghai municipal government (15520711200), and Marie
859 Skłodowska-Curie Actions (690958-MARSU-RISE-2015). The meteorological data are available at
860 <http://data.cma.cn/>. The socioeconomic data are collected from <http://www.stats.gov.cn/>.

861



References

- Abed, A.M., Kuisi, M.A., Khair, H.A.: Characterization of the Khamaseen (spring) dust in Jordan, Atmos. Environ. 43, 2868-2876, <https://doi.org/10.1016/j.atmosenv.2009.03.015>, 2009.
- AlKhatib, M. and Eisenhauer, A.: Calcium and strontium isotope fractionation during precipitation from aqueous solutions as a function of temperature and reaction rate; II. Aragonite. 209, 320-342, 2017.
- Al-Khashman, O. A.: Study of chemical composition in wet atmospheric precipitation in Eshidiya area, Jordan, Atmos. Environ. 39(33), 6175-6183, <https://doi.org/10.1016/j.atmosenv.2005.06.056>, 2005.
- Allen, H. M., Draper, D.C., Ayres, B.R., Ault, R., Bondy, A., Takahama, S., Modini, R.L., Baumann, K., Edgerton, E., and Knote, C.: Influence of crustal dust and sea spray supermicron particle concentrations and acidity on inorganic NO_3^- aerosol during the 2013 Southern Oxidant and Aerosol Study, Atmos. Chem. Phys., 15(18), 10669-10685, <https://www.atmos-chem-phys.net/15/10669/2015/>, 2015.
- Aloisi, I., G. Cai, C. Faleri, L. Navazio, D. Serafini-Fracassini, and S. Del Duca.: Spermine regulates pollen tube growth by modulating Ca^{2+} -dependent actin organization and cell wall structure, Front Plant Sci, 8, 1701, 2017.
- Antony Chen, L. W., B. G. Doddridge, R. R. Dickerson, J. C. Chow, P. K. Mueller, J. Quinn, and W. A. Butler.: Seasonal variations in elemental carbon aerosol, carbon monoxide and sulfur dioxide: Implications for sources, Geophys. Res. Lett., 28(9), 1711-1714, <https://doi.org/10.1029/2000GL012354>, 2001.
- Arimoto, R., R. Duce, D. Savoie, J. Prospero, R. Talbot, J. Cullen, U. Tomza, N. Lewis, and B. Ray.: Relationships among aerosol constituents from Asia and the North Pacific during PEM - West A, J. Geophys. Res., 101(D1), 2011-2023, <https://doi.org/10.1029/95JD01071>, 1996.
- Bao, G., Q. Ao, Q. Li, Y. Bao, Y. Zheng, X. Feng, and X. Ding.: Physiological Characteristics of *Medicago sativa* L. in Response to Acid Deposition and Freeze-Thaw Stress, Water Air Soil Poll., 228(9),



376, 2017.

Balasubramanian, R., Victor, T., Chun, N.: Chemical and statistical analysis of precipitation in Singapore.

Water Air Soil Poll. 130, 451-456, 2001.

Baumbach, G., Vogt, U.: Experimental determination of the effect of mountain-valley breeze circulation on air pollution in the vicinity of Freiburg. Atmos. Environ. 33, 4019-4027, [https://doi.org/10.1016/S1352-2310\(99\)00143-0](https://doi.org/10.1016/S1352-2310(99)00143-0), 1999.

Beniston.: Environmental change in mountains and uplands, 2016.

Bian, S., D. Li, D. Gao, J. Peng, Y. Dong, and W. Li.: Hydrometallurgical processing of lithium, potassium, and boron for the comprehensive utilization of Da Qaidam lake brine via natural evaporation and freezing, Hydrometallurgy, 173, 80-83, 2017.

Bowden, R. D., E. Davidson, K. Savage, C. Arabia, and P. Steudler.: Chronic nitrogen additions reduce total soil respiration and microbial respiration in temperate forest soils at the Harvard Forest, Forest Ecol Manag., 196(1), 43-56, 2004.

Cao, Y.-Z., S. Wang, G. Zhang, J. Luo, and S. Lu.: Chemical characteristics of wet precipitation at an urban site of Guangzhou, South China, Atmos. Res., 94(3), 462-469, <https://doi.org/10.1016/j.atmosres.2009.07.004>, 2009.

Cabello, M., Orza, J.A.G., Duenas, C., Liger, E., Gordo, E., Canete, S.: Back-trajectory analysis of African dust outbreaks at a coastal city in southern Spain: Selection of starting heights and assessment of African and concurrent Mediterranean contributions, Atmos. Environ., 140, 10-21, <https://doi.org/10.1016/j.atmosenv.2016.05.047>, 2016.

Chen, J., C. Li, Z. Ristovski, A. Milic, Y. Gu, M. S. Islam, S. Wang, J. Hao, H. Zhang, and C. He.: A review of biomass burning: Emissions and impacts on air quality, health and climate in China, Sci. Total



Environ., 579, 1000-1034, <https://doi.org/10.1016/j.scitotenv.2016.11.025>, 2017a.

Chen, J., G. Liu, Y. Kang, B. Wu, R. Sun, C. Zhou, and D. Wu.: Atmospheric emissions of F, As, Se, Hg, and Sb from coal-fired power and heat generation in China, Chemosphere, 90(6), 1925-1932, <https://doi.org/10.1016/j.chemosphere.2012.10.032>, 2013.

Chen, P., T. Wang, X. Lu, Y. Yu, M. Kasoar, M. Xie, and B. Zhuang.: Source apportionment of size-fractionated particles during the 2013 Asian Youth Games and the 2014 Youth Olympic Games in Nanjing, China, Sci. Total Environ., 579, 860-870, <https://doi.org/10.1016/j.scitotenv.2016.11.014>, 2017b.

Chen, Y., B. Luo, and S.-d. Xie.: Characteristics of the long-range transport dust events in Chengdu, Southwest China, Atmos. Environ., 122, 713-722, <https://doi.org/10.1016/j.atmosenv.2015.10.045>, 2015.

Cheng, Y.-q., and P. Zhang.: Regional patterns changes of Chinese grain production and response of commodity grain base in northeast China, Scientia Geographica Sinica, 25(5), 514, 2005.

Cheng, Y., G. Engling, K.-b. He, F.-k. Duan, Z.-y. Du, Y.-l. Ma, L.-l. Liang, Z.-f. Lu, J.-m. Liu, and M. Zheng.: The characteristics of Beijing aerosol during two distinct episodes: Impacts of biomass burning and fireworks, Environ. Pollut., 185, 149-157, <https://doi.org/10.1016/j.envpol.2013.10.037>, 2014.

Chen, Z.J., Chen, C.X., Liu, Y.Q., Lin, Z.S.: The background values and characteristics of soil elements in Fujian province. Environ. Monit. China, 8, 107-110, 1992.

Cong, Z., S. Kang, and K. Kawamura (2016), The long-range transport of atmospheric aerosols from South Asia to Himalayas, paper presented at EGU General Assembly Conference Abstracts.

Clemens, S.: Toxic metal accumulation, responses to exposure and mechanisms of tolerance in plants, 88, 1707-1719, 2006.

Dai, S., and D. Ren.: Fluorine concentration of coals in China-an estimation considering coal reserves,



Fuel, 85(7), 929-935, 2006.

Deshmukh, D. K., M. K. Deb, Y. I. Tsai, and S. L. Mkoma.: Water soluble ions in PM_{2.5} and PM₁ aerosols in Durg city, Chhattisgarh, India, Aerosol Air Qual. Res, 11, 696-708, 10.4209/aaqr.2011.03.0023, 2011.

Ding, X., L. Kong, C. Du, A. Zhanzakova, H. Fu, X. Tang, L. Wang, X. Yang, J. Chen, and T. Cheng.: Characteristics of size-resolved atmospheric inorganic and carbonaceous aerosols in urban Shanghai, Atmos. Environ., 167, 625-641, <https://doi.org/10.1016/j.atmosenv.2017.08.043>, 2017.

Dong, Z.W., Kang, S.C., Guo, J.M., Zhang, Q.G., Wang, X.J., Qi, D.H.: Composition and mixing states of brown haze particle over the Himalayas along two transboundary south-north transects, Atmos. Environ., 156, 24-35, <https://doi.org/10.1016/j.atmosenv.2017.02.029>, 2017.

Driscoll, C. T., K. M. Driscoll, M. J. Mitchell, and D. J. Raynal.: Effects of acidic deposition on forest and aquatic ecosystems in New York State, Environ. Pollut., 123(3), 327-336, [https://doi.org/10.1016/S0269-7491\(03\)00019-8](https://doi.org/10.1016/S0269-7491(03)00019-8), 2003.

Du, E.Z., Vries, W.D., Galloway, J.N., Hu, X.Y., Fang, J.Y.: Changes in wet nitrogen deposition in the United States between 1985 and 2012, Environ. Res. Lett., 9, 095004, <https://doi.org/10.1088/1748-9326/9/9/095004>, 2014.

Emmett, B.: The impact of nitrogen on forest soils and feedbacks on tree growth, in Forest Growth Responses to the Pollution Climate of the 21st Century, edited, pp. 65-74, Springer, 1999.

Engelbrecht, P. J., Moosmüller, H., Pincock, S., Jayanty, R.K.M., Lersch, T., Casuccio, G.: Technical note: Mineralogical, chemical, morphological, and optical interrelationships of mineral dust re-suspensions. Atmos. Chem. Phys. 16, 10809–10830, <https://www.atmos-chem-phys.net/16/10809/2016/>, 2016.

Fornaro, A., Gutz, I.G.R.: Wet deposition and related atmospheric chemistry in the São Paulo metropolis,



Brazil: part 2-contribution of formic and acetic acids. Atmos. Environ. 37, 117-128,
[https://doi.org/10.1016/S1352-2310\(02\)00885-3](https://doi.org/10.1016/S1352-2310(02)00885-3), 2003.

Fu, H., G. Shang, J. Lin, Y. Hu, Q. Hu, L. Guo, Y. Zhang, and J. Chen.: Fractional iron solubility of aerosol particles enhanced by biomass burning and ship emission in Shanghai, East China, Sci. Total Environ., 481, 377-391, <https://doi.org/10.1016/j.scitotenv.2014.01.118>, 2014.

Fu, H.B., Chen, J.M.: Formation, features and controlling strategies of severe haze-fog pollutions in China, Sci. Total Environ., 578, 121-138, <https://doi.org/10.1016/j.scitotenv.2016.10.201>, 2016.

Garland, J.A.: Dry and wet removal of sulphur from the atmosphere, Sulfur in the Atmosphere, 349-362, 1978.

Gerson, J. R., C. T. Driscoll, and K. M. Roy.: Patterns of nutrient dynamics in Adirondack lakes recovering from acid deposition, Ecol. Appl., 26(6), 1758-1770, 2016.

Glavas, S., Moschonas, N.: Origin of observed acidic-alkaline rains in a wet-only precipitation study in a Mediterranean coastal site, Patras, Greece. Atmos. Environ. 36, 3089-3099,
[https://doi.org/10.1016/S1352-2310\(02\)00262-5](https://doi.org/10.1016/S1352-2310(02)00262-5), 2002.

Gottwald, M., Bovensmann, H.: SCIAMACHY: Exploring the Changing Earth's Atmosphere, first ed. Springer (ISBN 978-9-481-9895-5), 2011.

Grythe, H., J. Ström, R. Krejci, P. Quinn, and A. Stohl.: A review of sea-spray aerosol source functions using a large global set of sea salt aerosol concentration measurements, Atmos. Chem. Phys., 14(3), 1277, <https://www.atmos-chem-phys.net/14/1277/2014/>, 2014.

Gu, J., Pitz, M., Schnelle-Kreis, J., Diemer, J., Reller, A., Zimmermann, R., Soentgen, J., Staelzel, M., Wichmann, H.E., Peters, A., Cyrys, J.: Source apportionment of ambient particles: comparison of positive matrix factorization analysis applied to particle size distribution and chemical composition data.



Atmos. Environ. 45, 1849-1857, <https://doi.org/10.1016/j.atmosenv.2011.01.009>, 2011.

Gu, Y., H. Liao, and J. Bian.: Summertime nitrate aerosol in the upper troposphere and lower stratosphere over the Tibetan Plateau and the South Asian summer monsoon region, Atmos. Chem. Phys., 16(11), 6641-6663, <https://doi.org/10.5194/acp-16-6641-2016>, 2016.

Gupta, D., H.-J. Eom, H.-R. Cho, and C.-U. Ro.: Hygroscopic behavior of NaCl-MgCl₂ mixture particles as nascent sea-spray aerosol surrogates and observation of efflorescence during humidification, Atmos. Chem. Phys., 15(19), 11273-11290, <https://doi.org/10.5194/acp-15-11273-2015>, 2015.

Hao, G.J., Zhou, J.Q., Fang, H.L.: Applicability of AB-DTPA method for determining the available content of multi-element in typical soils in China, Acta Agr. Shanghai (in Chinese), 32, 100-107, 2016.

Hua, S., H. Tian, K. Wang, C. Zhu, J. Gao, Y. Ma, Y. Xue, Y. Wang, S. Duan, and J. Zhou.: Atmospheric emission inventory of hazardous air pollutants from China's cement plants: Temporal trends, spatial variation characteristics and scenario projections, Atmos. Environ., 128, 1-9, <https://doi.org/10.1016/j.atmosenv.2015.12.056>, 2016.

Hunová, I., Maznová, J., Kurfürst, P.: Trends in atmospheric deposition fluxes of sulphur and nitrogen in Czech forests, Environ. Pollut., 184, 668-675, <https://doi.org/10.1016/j.envpol.2013.05.013>, 2014.

Ito, M., Mitchell, M., Driscoll, C.T.: Spatial patterns of precipitation quantity and chemistry and air temperature in the Adirondack region of New York. Atmos. Environ. 36, 1051-1062, [https://doi.org/10.1016/S1352-2310\(01\)00484-8](https://doi.org/10.1016/S1352-2310(01)00484-8), 2002.

Jia, Y., G. Yu, N. He, X. Zhan, H. Fang, W. Sheng, Y. Zuo, D. Zhang, and Q. Wang.: Spatial and decadal variations in inorganic nitrogen wet deposition in China induced by human activity, Scientific Reports, 4, <https://doi.org/10.1038/srep03763>, 2014.

Jiang, Z., Y. Lian, and X. Qin.: Rocky desertification in Southwest China: impacts, causes, and



- restoration, *Earth-Science Reviews*, 132, 1-12, <https://doi.org/10.1016/j.earscirev.2014.01.005>, 2014.
- Kang, Y., M. Liu, Y. Song, X. Huang, H. Yao, X. Cai, H. Zhang, L. Kang, X. Liu, and X. Yan.: High-resolution ammonia emissions inventories in China from 1980 to 2012, *Atmos. Chem. Phys.*, 16(4), 2043-2058, <https://doi.org/10.5194/acp-16-2043-2016>, 2016.
- Kang, L.T., Huang, J.P., Chen, S.Y., Wang, X.: Long-term trends of dust events over Tibetan Plateau during 1961–2010, *Atmos. Environ.*, 125, 188-198, <https://doi.org/10.1016/j.atmosenv.2015.10.085>, 2016.
- Kabatas, B., Unal, A., Pierce, R.B., Kindap, T., Pozzoli, L.: The contribution of Saharan dust in PM₁₀ concentration levels in Anatolian Peninsula of Turkey, *Sci. Total Environ.*, 488-489, 413-421, <https://doi.org/10.1016/j.scitotenv.2013.12.045>, 2014.
- Kchih, H., C. Perrino, and S. Cherif.: Investigation of desert dust contribution to source apportionment of PM₁₀ and PM_{2.5} from a southern Mediterranean coast, *Aerosol Air Qual. Res.* 15(2), 454-464, 10.4209/aaqr.2014.10.0255, 2015.
- Keene, W. C., Pszenny, A. A. P., Galloway, J. N., and Hawley, M. E.: Sea-salt corrections and interpretation of constituent ratios in marine precipitation, *J. Geophys. Res.-Atmos.*, 91, 6647–6658, <https://doi.org/10.1029/JD091iD06p06647>, 1986.
- Kong, S., Y. Ji, B. Lu, L. Chen, B. Han, Z. Li, and Z. Bai.: Characterization of PM₁₀ source profiles for fugitive dust in Fushun-a city famous for coal, *Atmos. Environ.*, 45(30), 5351-5365, <https://doi.org/10.1016/j.atmosenv.2011.06.050>, 2011.
- Kobbing, J.F., Patuzzi, F., Baratieri, M., Beckmann, V., Thevs, N., Zerbe, S.: Economic evaluation of common reed potential for energy production: a case study in Wuliangshuai Lake (Inner Mongolia, China). *Biomass Bioenerg.* 70, 315-329, 2014.



Kulshrestha, U.C., Sarkar, A.K., Srivastava, S.S., Parashar, D.C.: Wet-only and bulk deposition studies at New Delhi (India). *Water Air Soil Pollut.*, 85, 2137–2142, 1995.

Kuribayashi, M., T. Ohara, Y. Morino, I. Uno, J.-i. Kurokawa, and H. Hara.: Long-term trends of sulfur deposition in East Asia during 1981-2005, *Atmos. Environ.*, 59, 461-475, <https://doi.org/10.1016/j.atmosenv.2012.04.060>, 2012.

Kuang, F.H., Liu, X.J., Zhu, B., Shen, J., Pan, Y., Su, M.: Wet and dry nitrogen deposition in the central Sichuan Basin of China, *Atmos. Environ.* 143, 39-50, <https://doi.org/10.1016/j.atmosenv.2016.08.032>, 2016.

Lawson, D.R., Winchester, J.W.: A standard crustal aerosol as a reference for elemental enrichment factors, *Atmos. Environ.* 13, 925-930, 1979.

Larssen, T., and G. Carmichael.: Acid rain and acidification in China: the importance of base cation deposition, *Environ. Pollut.*, 110(1), 89-102, [https://doi.org/10.1016/S0269-7491\(99\)00279-1](https://doi.org/10.1016/S0269-7491(99)00279-1), 2000.

Larssen, T., H. M. Seip, A. Semb, J. Mulder, I. P. Muniz, R. D. Vogt, E. Lydersen, V. Angell, T. Dagang, and O. Eilertsen.: Acid deposition and its effects in China: an overview, *Environ. Sci. Poli.*, 2(1), 9-24, 1999.

Leng, Q.M., Cui, J., Zhou, F.W., Du, K., Zhang, L.Y., Fu, C., Liu, Y., Wang, H.B., Shi, G.M., Gao, M., Yang, F.M., He, D.Y.: Wet-only deposition of atmospheric inorganic nitrogen and associated isotopic characteristics in a typical mountain area, southwestern China, *Sci. Environ. Total*, 616, 55-63, <https://doi.org/10.1016/j.scitotenv.2017.10.240>, 2018.

Le Bolloch, O., Guerzoni, S.: Acid and alkaline deposition in precipitation on the western coast of Sardinia, Central Mediterranean (40 N, 81 E). *Water Air Soil Poll.* 85, 2155-2160, 1995.

Li, C.L., Kang, S.C., Zhang, Q.G., Kaspari, S.: Major ionic composition of precipitation in the Nam Co



region, Central Tibetan Plateau. Atmos. Res. 85, 351–360,

<https://doi.org/10.1016/j.atmosres.2007.02.006>, 2007.

Li, L., Q. Tan, Y. Zhang, M. Feng, Y. Qu, J. An, and X. Liu.: Characteristics and source apportionment of PM_{2.5} during persistent extreme haze events in Chengdu, southwest China, Environ. Pollut., 230, 718-729, <https://doi.org/10.1016/j.envpol.2017.07.029>, 2017a.

Li, R., L. Cui, J. Li, A. Zhao, H. Fu, Y. Wu, L. Zhang, L. Kong, and J. Chen.: Spatial and temporal variation of particulate matter and gaseous pollutants in China during 2014–2016, Atmos. Environ., 161, 235-246, <https://doi.org/10.1016/j.atmosenv.2017.05.008>, 2017b.

Li, X., L. Wang, D. Ji, T. Wen, Y. Pan, Y. Sun, and Y. Wang.: Characterization of the size-segregated water-soluble inorganic ions in the Jing-Jin-Ji urban agglomeration: Spatial/temporal variability, size distribution and sources, Atmos. Environ., 77, 250-259, <https://doi.org/10.1016/j.atmosenv.2013.03.042>, 2013.

Li, Y., J. Meng, J. Liu, Y. Xu, D. Guan, W. Tao, Y. Huang, and S. Tao.: Interprovincial reliance for improving air quality in China: a case study on black carbon aerosol, Environ. Sci. Technol., 50(7), 4118-4126, 10.1021/acs.est.5b05989, 10.1021/acs.est.5b05989, 2016.

Li, R., Li, J.L., Cui, L.L., Wu, Y., Fu, H.B., Chen, J.M., Chen, M.D.: Atmospheric emissions of Cu and Zn from coal combustion in China: Spatio-temporal distribution, human health effects, and short-term prediction, Environ. Pollut., 229, 724-734, <https://doi.org/10.1016/j.envpol.2017.05.068>, 2017.

Li, Z.Y., Wang, Z.L., Li, R.J., Xu, Q.H.: The analysis of element content in the soil of 29 provinces/municipality/autonomous region in China, Shanghai agriculture technology (in Chinese), 1992.

Li, Z., Ma, Z., vander Kuijp, T., Yuan, Z.W., Huang, L.: A review of soil heavy metal pollution from mines in China: Pollution and health risk assessment, Sci. Total Environ. 468-469, 843-853,



<https://doi.org/10.1016/j.scitotenv.2018.06.068>, 2014.

Lim, B., T. Jickells, and T. Davies.: Sequential sampling of particles, major ions and total trace metals in wet deposition, *Atmospheric Environment. Part A. General Topics*, 25(3-4), 745-762, 1991.

Link, M. F., J. Kim, G. Park, T. Lee, T. Park, Z. B. Babar, K. Sung, P. Kim, S. Kang, and J. S. Kim.: Elevated production of $\text{NH}_4\text{-NO}_3$ from the photochemical processing of vehicle exhaust: Implications for air quality in the Seoul Metropolitan Region, *Atmos. Environ.*, 156, 95-101, <https://doi.org/10.1016/j.atmosenv.2017.02.031>, 2017.

Liu, F., S. Beirle, Q. Zhang, B. Zheng, D. Tong, and K. He.: NO_x emission trends over Chinese cities estimated from OMI observations during 2005 to 2015, *Atmos. Chem. Phys.*, 17(15), 9261-9275, <https://doi.org/10.5194/acp-17-9261-2017>, 2017.

Liu, F., Q. Zhang, D. Tong, B. Zheng, M. Li, H. Huo, and K. He.: High-resolution inventory of technologies, activities, and emissions of coal-fired power plants in China from 1990 to 2010, *Atmos. Chem. Phys.*, 15(23), 13299-13317, <https://doi.org/10.5194/acp-15-13299-2015>, 2015a.

Liu, Y. W., Ri, X., Wang, Y. S., Pan, Y. P., Piao, S. L.: Wet deposition of atmospheric inorganic nitrogen at five remote sites in the Tibetan Plateau, *Atmos. Chem. Phys.*, 15, 11683-11700, <https://doi.org/10.5194/acp-15-11683-2015>, 2015b.

Liu, L., Zhang, X.Y., Wang, S.Q., Zhang, W.T., Lu, X.H.: Bulk sulfur deposition in China, *Atmos. Environ.*, 135, 41-49, <https://doi.org/10.1016/j.atmosenv.2016.04.003>, 2016a.

Liu, P.F., Zhang, C., Mu, Y., Liu, C.T., Xue, C.Y., Ye, C., Liu, J.F., Zhang, Y.Y., Zhang, H.X.: The possible contribution of the periodic emissions from farmers' activities in the North China Plain to atmospheric water-soluble ions in Beijing, *Atmos. Chem. Phys.*, 16, 10097-10109, <https://doi.org/10.5194/acp-16-10097-2016>, 2016b.



Liu, P.F., Zhang, C.L., Xue, C.Y., Mu, Y.J., Liu, J.F., Zhang, Y.Y., Tian, D., Ye, C., Zhang, H.X., Guan, J.: The contribution of residential coal combustion to atmospheric PM_{2.5} in northern China during winter, Atmos. Chem. Phys., 17, 11503–11520, <https://doi.org/10.5194/acp-17-11503-2017>, 2017.

Liu, X., L. Duan, J. Mo, E. Du, J. Shen, X. Lu, Y. Zhang, X. Zhou, C. He, and F. Zhang.: Nitrogen deposition and its ecological impact in China: an overview, Environ. Pollut., 159(10), 2251-2264, <https://doi.org/10.1016/j.envpol.2010.08.002>, 2011.

Liu, X., X. Ju, Y. Zhang, C. He, J. Kopsch, and Z. Fusuo.: Nitrogen deposition in agroecosystems in the Beijing area, Agr. Ecosyst. Environ., 113(1), 370-377, 2006.

Liu, X., Y. Zhang, W. Han, A. Tang, J. Shen, Z. Cui, P. Vitousek, J. W. Erisman, K. Goulding, and P. Christie.: Enhanced nitrogen deposition over China, Nature, 494(7438), 459, <https://doi.org/10.1038/nature11917>, 2013.

Lu, X., L. Y. Li, N. Li, G. Yang, D. Luo, and J. Chen.: Chemical characteristics of spring precipitation of Xi'an city, NW China, Atmos. Environ., 45(28), 5058-5063, <https://doi.org/10.1016/j.atmosenv.2011.06.026>, 2011.

Lu, X., Q. Mao, F. S. Gilliam, Y. Luo, and J. Mo.: Nitrogen deposition contributes to soil acidification in tropical ecosystems, Global Change Biol., 20(12), 3790-3801, <https://doi.org/10.1111/gcb.12665>, 2014.

Lu, Z., D. G. Streets, Q. Zhang, S. Wang, G. R. Carmichael, Y. F. Cheng, C. Wei, M. Chin, T. Diehl, and Q. Tan.: Sulfur dioxide emissions in China and sulfur trends in East Asia since 2000, Atmos. Chem. Phys., 10(13), 6311-6331, <https://doi.org/10.5194/acp-10-6311-2010>, 2010.

Luo, X.S., Xue, Y., Wang, Y.L., Cang, L., Xu, B., Ding, J.: Source identification and apportionment of heavy metals in urban soil profiles, Chemosphere., 127, 152-157, <https://doi.org/10.1016/j.chemosphere.2015.01.048>, 2015.



Lyu, X., N. Chen, H. Guo, L. Zeng, W. Zhang, F. Shen, J. Quan, and N. Wang.: Chemical characteristics and causes of airborne particulate pollution in warm seasons in Wuhan, central China, Atmos. Chem. Phys., 16(16), 10671-10687, <https://doi.org/10.5194/acp-16-10671-2016>, 2016.

Lyu, Y., Z. Qu, L. Liu, L. Guo, Y. Yang, X. Hu, Y. Xiong, G. Zhang, M. Zhao, and B. Liang.: Characterization of dustfall in rural and urban sites during three dust storms in northern China, 2010, Aeolian Res., 28, 29-37, 2017.

McGlade, C., Ekins, P.: The geographical distribution of fossil fuels unused when limiting global warming to 2 °C, Nature, 517, 187-190, <https://doi.org/10.1038/nature14016>, 2015.

Müller, W. E., E. Tolba, Q. Feng, H. C. Schröder, J. S. Markl, M. Kokkinopoulou, and X. Wang.: Amorphous Ca²⁺ polyphosphate nanoparticles regulate the ATP level in bone-like SaOS-2 cells, J. Cell Sci., 128(11), 2202-2207, 2015.

Migliavacca, D., E. Teixeira, F. Wiegand, A. Machado, and J. Sanchez.: Atmospheric precipitation and chemical composition of an urban site, Guaíba hydrographic basin, Brazil, Atmos. Environ., 39(10), 1829-1844, <https://doi.org/10.1016/j.atmosenv.2004.12.005>, 2005.

Mikhailova, E., M. Goddard, C. Post, M. Schlautman, and J. Galbraith.: Potential contribution of combined atmospheric Ca²⁺ and Mg²⁺ wet deposition within the continental US to soil inorganic carbon sequestration, Pedosphere, 23(6), 808-814, 2013.

National Bureau of Statistics of China, 2010-2016 (Chinese).

Négrel, P., C. Guerrot, and R. Millot.: Chemical and strontium isotope characterization of precipitation in France: influence of sources and hydrogeochemical implications, Isot. Environ. Health., 43(3), 179-196, 2007.

Nayebare, S. R., O. S. Aburizaiza, H. A. Khwaja, A. Siddique, M. M. Hussain, J. Zeb, F. Khatib, D. O.



Carpenter, and D. R. Blake.: Chemical Characterization and Source Apportionment of PM_{2.5} in Rabigh, Saudi Arabia, *Aerosol Air Qual Re.*, 16(12), 3114-3129, 10.4209/aaqr.2015.11.0658, 2016.

Niu, H.W., He, Y.Q., Lu, X.X., Shen, J., Du, J.K., Zhang, T., Pu, T., Xin, H.J., Chang, L.: Chemical composition of precipitation in the Yulong Snow Mountain region, Southwestern China. *Atmos. Res.* 144, 195-206, <https://doi.org/10.1016/j.atmosres.2014.03.010>, 2014.

Okuda, T., T. Iwase, H. Ueda, Y. Suda, S. Tanaka, Y. Dokiya, K. Fushimi, and M. Hosoe.: Long-term trend of chemical constituents in precipitation in Tokyo metropolitan area, Japan, from 1990 to 2002, *Sci. Total Environ.* 339(1), 127-141, <https://doi.org/10.1016/j.scitotenv.2004.07.024>, 2005.

Wang, W.X., Xu, P.J.: Research Progress in Precipitation Chemistry in China, *Progress in Chemistry*, Z1, 2009.

Padoan, E., Ajmone-Marsan, F., Querol, X., Amato, F.: An empirical model to predict road dust emissions based on pavement and traffic characteristics, *Environ. Pollut.* 237, 713-720, <https://doi.org/10.1016/j.envpol.2017.10.115>, 2017.

Pan, Y. P., Wang, Y. S., Tang, G. Q., Du, W.: Spatial distribution and temporal variations of atmospheric sulfur deposition in Northern China: insights into the potential acidification risks, *Atmos. Chem. Phys.* 1675-1688, <https://doi.org/10.5194/acp-13-1675-2013>, 2013.

Prather, K. A., T. H. Bertram, V. H. Grassian, G. B. Deane, M. D. Stokes, P. J. DeMott, L. I. Aluwihare, B. P. Palenik, F. Azam, and J. H. Seinfeld.: Bringing the ocean into the laboratory to probe the chemical complexity of sea spray aerosol, *P. Natl. Acad. Sci. USA.* 110(19), 7550-7555, <https://doi.org/10.1073/pnas.1300262110>, 2013.

Pu, W., W. Quan, Z. Ma, X. Shi, X. Zhao, L. Zhang, Z. Wang, and W. Wang.: Long-term trend of chemical composition of atmospheric precipitation at a regional background station in Northern China, *Sci. Total*



Environ., 580, 1340-1350, <https://doi.org/10.1016/j.scitotenv.2016.12.097>, 2017.

Qiao, T., M. Zhao, G. Xiu, and J. Yu.: Seasonal variations of water soluble composition (WSOC, Hulis and WSIs) in PM₁ and its implications on haze pollution in urban Shanghai, China, Atmos. Environ., 123, 306-314, <https://doi.org/10.1016/j.atmosenv.2015.03.010>, 2015.

Qiao, X., Du, J., Kota, S.H., Ying, Q., Xiao, W.Y., Tang, Y.: Wet deposition of sulfur and nitrogen in Jiuzhaigou National Nature Reserve, Sichuan, China during 2015-2016: Possible effects from regional emission reduction and local tourist activities. 233, 267-277. Environ. Pollut. 233, 267-277, <https://doi.org/10.1016/j.envpol.2017.08.041>, 2018.

Rao, W., G. Han, H. Tan, and S. Jiang.: Chemical and Sr isotopic compositions of precipitation on the Ordos Desert Plateau, Northwest China, Environ. Earth Sci., 74(7), 5759-5771, 2015.

Ren, D., F. Zhao, S. Dai, J. Zhang, and K. Luo.: Trace Element Geochemical in Coal, edited, Science Press, Beijing, China, 2006.

Russell, K. M., J. N. Galloway, S. A. Macko, J. L. Moody, and J. R. Scudlark.: Sources of nitrogen in wet deposition to the Chesapeake Bay region, Atmos. Environ., 32(14), 2453-2465, [https://doi.org/10.1016/S1352-2310\(98\)00044-2](https://doi.org/10.1016/S1352-2310(98)00044-2), 1998.

Seinfeld, J. H.: Atmospheric Chemistry and Physics of Air Pollution John Wiley & Sons, Inc., New York, 50-51, 1986.

Shen, Z., J. Sun, J. Cao, L. Zhang, Q. Zhang, Y. Lei, J. Gao, R.-J. Huang, S. Liu, and Y. Huang.: Chemical profiles of urban fugitive dust PM_{2.5} samples in Northern Chinese cities, Sci. Total Environ., 569, 619-626, <https://doi.org/10.1016/j.scitotenv.2016.06.156>, 2016.

Shi, C.W., Zhao, L.Z., Guo, X.B., Gao, S., Yang, J.P., Li, J.H.: The distribution characteristic and influential factors of background values for elements in Shanxi province, Agro-environmental Protection,



15, 24-28, 1996.

Shi, G.L., Liu, G.R., Peng, X., Wang, Y.N., Tian, Y.Z., Wang, W., Feng, Y.C.: A comparison of multiple combined models for source apportionment, including the PCA/MLR-CMB, UNMIX-CMB and PMF-CMB Models, *Aerosol Air Qual. R.*, 14, 2040-2050, 2014.

Sickles II, J.E., Shadwick, D.S.: Air quality and atmospheric deposition in the eastern US: 20 years of change, *Atmos. Chem. Phys.*, 15, 173-197, <https://doi.org/10.5194/acp-15-173-2015>, 2015.

Simkin, S. M., E. B. Allen, W. D. Bowman, C. M. Clark, J. Belnap, M. L. Brooks, B. S. Cade, S. L. Collins, L. H. Geiser, and F. S. Gilliam.: Conditional vulnerability of plant diversity to atmospheric nitrogen deposition across the United States, *P. Natl. Acad. Sci. USA.*, 113(15), 4086-4091, <https://doi.org/10.1073/pnas.1515241113>, 2016.

Singh, A., Agrawal, M.: Acid rain and its ecological consequences. *J. Environ. Biol.* 29, 15-24, 2008.

Smith, S. J., J. v. Aardenne, Z. Klimont, R. J. Andres, A. Volke, and S. Delgado Arias.: Anthropogenic sulfur dioxide emissions: 1850–2005, *Atmos. Chem. Phys.*, 11(3), 1101-1116, <https://doi.org/10.5194/acp-11-1101-2011>, 2011.

Song, F., Gao, Y.: Chemical characteristics of precipitation at metropolitan Newark in the US East Coast. *Atmos. Environ.* 43, 4903-4913, <https://doi.org/10.1016/j.atmosenv.2009.07.024>, 2009.

Song, H., K. Zhang, S. Piao, and S. Wan.: Spatial and temporal variations of spring dust emissions in northern China over the last 30 years, *Atmos. Environ.*, 126, 117-127, <https://doi.org/10.1016/j.atmosenv.2015.11.052>, 2016.

Song, Y., Y. Zhang, S. Xie, L. Zeng, M. Zheng, L. G. Salmon, M. Shao, and S. Slanina.: Source apportionment of PM_{2.5} in Beijing by positive matrix factorization, *Atmos. Environ.*, 40(8), 1526-1537, <https://doi.org/10.1016/j.atmosenv.2005.10.039>, 2006.



Sun, L., L. Li, Z. Chen, J. Wang, and Z. Xiong.: Combined effects of nitrogen deposition and biochar application on emissions of N₂O, CO₂ and NH₃ from agricultural and forest soils, *Soil Sci. Plant Nutr.*, 60(2), 254-265, 2014.

Sun, S.D., Jiang, W., Gao, W.D.: Vehicle emission trends and spatial distribution in Shandong province, China, from 2000 to 2014, *Atmos. Environ.*, 147, 190-199, <https://doi.org/10.1016/j.atmosenv.2016.09.065>, 2016.

Song, M.-L., Zhang, W., Wang, S.-H.: Inflection point of environmental Kuznets curve in Mainland China. *Energy Policy* 57, 14-20., 2013.

Song, L., Kuang, F.H., Skiba, U., Zhu, B., Liu, X.J., Levy, P., Dore, A., Fowler, D.: Bulk deposition of organic and inorganic nitrogen in southwest China from 2008 to 2013, *Environ. Pollut.*, 227, 157-166, <https://doi.org/10.1016/j.envpol.2017.04.031>, 2017.

Tai, A. P., L. J. Mickley, and D. J. Jacob.: Correlations between fine particulate matter (PM_{2.5}) and meteorological variables in the United States: Implications for the sensitivity of PM_{2.5} to climate change, *Atmos. Environ.*, 44(32), 3976-3984, <https://doi.org/10.1016/j.atmosenv.2010.06.060>, 2010.

Tao, J., L. Zhang, R. Zhang, Y. Wu, Z. Zhang, X. Zhang, Y. Tang, J. Cao, and Y. Zhang.: Uncertainty assessment of source attribution of PM_{2.5} and its water-soluble organic carbon content using different biomass burning tracers in positive matrix factorization analysis-A case study in Beijing, China, *Sci. Total Environ.*, 543, 326-335, <https://doi.org/10.1016/j.scitotenv.2015.11.057>, 2016.

Teinilä, K., A. Frey, R. Hillamo, H. C. Tülp, and R. Weller.: A study of the sea-salt chemistry using size-segregated aerosol measurements at coastal Antarctic station Neumayer, *Atmos. Environ.*, 96, 11-19, <https://doi.org/10.1016/j.atmosenv.2014.07.025>, 2014.

Teng, X., Q. Hu, L. Zhang, J. Qi, J. Shi, H. Xie, H. Gao, and X. Yao.: Identification of major sources of



atmospheric NH₃ in an urban environment in northern China during wintertime, *Environ. Sci. Technol.*, 51, 6839–6848, [10.1021/acs.est.7b00328](https://doi.org/10.1021/acs.est.7b00328), 2017.

Tian, H., J. Gao, L. Lu, D. Zhao, K. Cheng, and P. Qiu.: Temporal trends and spatial variation characteristics of hazardous air pollutant emission inventory from municipal solid waste incineration in China, *Environ. Sci. Technol.*, 46(18), 10364-10371, [10.1021/es302343s](https://doi.org/10.1021/es302343s), 2012.

Tian, H., K. Liu, J. Hao, Y. Wang, J. Gao, P. Qiu, and C. Zhu.: Nitrogen oxides emissions from thermal power plants in China: Current status and future predictions, *Environ. Sci. Technol.*, 47(19), 11350-11357, [10.1021/es402202d](https://doi.org/10.1021/es402202d), 2013.

Tian, H., K. Liu, J. Zhou, L. Lu, J. Hao, P. Qiu, J. Gao, C. Zhu, K. Wang, and S. Hua.: Atmospheric Emission Inventory of Hazardous Trace Elements from China's Coal-Fired Power Plants Temporal Trends and Spatial Variation Characteristics, *Environ. Sci. Technol.*, 48(6), 3575-3582, [10.1021/es404730j](https://doi.org/10.1021/es404730j), 2014.

Turekian, K. K.: *Oceans*, Prentice-Hall, New Jersey, United States, 1968.

Tsai, Y.I., Hsieh, L.Y., Kuo, S.C., Chen, C.L., Wu, P.L.: Seasonal and rainfall-type variations in inorganic ions and dicarboxylic acids and acidity of wet deposition samples collected from subtropical East Asia. *Atmos. Environ.* 45, 3535-3547, <https://doi.org/10.1016/j.atmosenv.2011.04.001>, 2011.

Vašát, R., L. Pavlů, L. Borůvka, V. Tejnecký, and A. Nikodem.: Modelling the impact of acid deposition on forest soils in north Bohemian Mountains with two dynamic models: The Very Simple Dynamic Model (VSD) and the Model of Acidification of Groundwater in Catchments (MAGIC), *Soil Water Res.*, 10(1), 10-18, 2015.

Velthof, G., J. Lesschen, J. Webb, S. Pietrzak, Z. Miatkowski, M. Pinto, J. Kros, and O. Oenema.: The impact of the Nitrates Directive on nitrogen emissions from agriculture in the EU-27 during 2000-2008,



Sci. Total Environ., 468, 1225-1233, <https://doi.org/10.1016/j.scitotenv.2013.04.058>, 2014.

Wang, F.Y., Liu, R.J., Lin, X.G., Zhou, J.M.: Arbuscular mycorrhizal status of wild plants in saline-alkaline soils of the Yellow River Delta. *Mycorrhiza* 14, 133-137, 2004.

Wang, H., J. An, M. Cheng, L. Shen, B. Zhu, Y. Li, Y. Wang, Q. Duan, A. Sullivan, and L. Xia.: One year online measurements of water-soluble ions at the industrially polluted town of Nanjing, China: Sources, seasonal and diurnal variations, *Chemosphere*, 148, 526-536, <https://doi.org/10.1016/j.chemosphere.2016.01.066>, 2016a.

Wang, K., H. Tian, S. Hua, C. Zhu, J. Gao, Y. Xue, J. Hao, Y. Wang, and J. Zhou.: A comprehensive emission inventory of multiple air pollutants from iron and steel industry in China: temporal trends and spatial variation characteristics, *Sci. Total Environ.*, 559, 7-14, <https://doi.org/10.1016/j.scitotenv.2016.03.125>, 2016b.

Wang, S., K. Luo, X. Wang, and Y. Sun (2016c), Estimate of sulfur, arsenic, mercury, fluorine emissions due to spontaneous combustion of coal gangue: An important part of Chinese emission inventories, *Environ. Pollut.*, 209, <https://doi.org/10.1016/j.envpol.2015.11.026>, 107-113.

Wang, Y., R. Wang, J. Ming, G. Liu, T. Chen, X. Liu, H. Liu, Y. Zhen, and G. Cheng (2016d), Effects of dust storm events on weekly clinic visits related to pulmonary tuberculosis disease in Minqin, China, *Atmos. Environ.*, 127, <https://doi.org/10.1016/j.atmosenv.2015.12.041>, 205-212.

Wang, Q.: Effects of urbanisation on energy consumption in China, *Energ. Policy*, 65, 332-339, 2014.

Wang, Q., G. Zhuang, K. Huang, T. Liu, C. Deng, J. Xu, Y. Lin, Z. Guo, Y. Chen, and Q. Fu.: Probing the severe haze pollution in three typical regions of China: Characteristics, sources and regional impacts, *Atmos. Environ.*, 120, 76-88, <https://doi.org/10.1016/j.atmosenv.2015.08.076>, 2015a.

Wang, X., W. Pu, J. Shi, J. Bi, T. Zhou, X. Zhang, and Y. Ren.: A comparison of the physical and optical



properties of anthropogenic air pollutants and mineral dust over Northwest China, *Acta Meteorol Sin.*, 29(2), 180-200, 2015b.

Wang, Y., Y. Xue, H. Tian, J. Gao, Y. Chen, C. Zhu, H. Liu, K. Wang, S. Hua, and S. Liu.: Effectiveness of temporary control measures for lowering PM_{2.5} pollution in Beijing and the implications, *Atmos. Environ.*, 157, 75-83, <https://doi.org/10.1016/j.atmosenv.2017.03.017>, 2017.

Wei, F. S., Chen, J. S., Wu, Y. Y., Zheng, C.J.: The study of background value in soil across China. *Environ. Sci.*, 12, 12-20, 1991 (in Chinese).

Wei, F.S., Yang, G.Z., Jiang, D.Z., Liu, Z.H., Sun, B.M.: The basic statistics and characteristics of soil elements in China. *Environ. Moni. China.*, 7, 1-6, 1991 (in Chinese).

Wu, J., Li, P., Qian, H., Duan, Z., Zhang, X.: Using correlation and multivariate statistical analysis to identify hydrogeochemical processes affecting the major ion chemistry of waters: a case study in Laoheba phosphorite mine in Sichuan, China, *Arab. J. Geosci.*, 7, 3973–3982, 2014.

Wu, Q., and G. Han.: Sulfur isotope and chemical composition of the precipitation at the Three Gorges Reservoir, *Atmos. Res.*, 155, 130-140, <https://doi.org/10.1016/j.atmosres.2014.11.020>, 2015.

Wu, J., G. Liang, D. Hui, Q. Deng, X. Xiong, Q. Qiu, J. Liu, G. Chu, G. Zhou, and D. Zhang.: Prolonged acid rain facilitates soil organic carbon accumulation in a mature forest in Southern China, *Sci. Total Environ.*, 544, 94-102, <https://doi.org/10.1016/j.scitotenv.2015.11.025>, 2016a.

Wu, X.M., Wu, Y., Zhang, S.J., Liu, H., Fu, L.X., Hao, J.M.: Assessment of vehicle emission programs in China during 1998-2013: achievement, challenges and implications, *Environ. Pollut.*, 214, 556-567, <https://doi.org/10.1016/j.envpol.2016.04.042>, 2016b.

Xiao, H.W., H.-Y. Xiao, A.-M. Long, Y.-L. Wang, and C.-Q. Liu.: Sources and meteorological factors that control seasonal variation of $\delta^{34}\text{S}$ values in precipitation, *Atmos. Res.*, 149, 154-165,



<https://doi.org/10.1016/j.atmosres.2014.06.003>, 2014.

Xing, J., J. Song, H. Yuan, X. Li, N. Li, L. Duan, X. Kang, and Q. Wang.: Fluxes, seasonal patterns and sources of various nutrient species (nitrogen, phosphorus and silicon) in atmospheric wet deposition and their ecological effects on Jiaozhou Bay, North China, *Sci. Total Environ.*, 576, 617-627,

<https://doi.org/10.1016/j.scitotenv.2016.10.134>, 2017.

Xu, P., Y. Liao, Y. Lin, C. Zhao, C. Yan, M. Cao, G. Wang, and S. Luan.: High-resolution inventory of ammonia emissions from agricultural fertilizer in China from 1978 to 2008, *Atmos. Chem. Phys.*, 16(3), 1207-1218, <https://doi.org/10.5194/acp-16-1207-2016>, 2016.

Xu, W., X. Luo, Y. Pan, L. Zhang, A. Tang, J. Shen, Y. Zhang, K. Li, Q. Wu, and D. Yang.: Quantifying atmospheric nitrogen deposition through a nationwide monitoring network across China, *Atmos. Chem. Phys.*, 15(21), 12345-12360, <https://doi.org/10.5194/acp-15-12345-2015>, 2015.

Yan, W., E. Mayorga, X. Li, S. P. Seitzinger, and A. Bouwman.: Increasing anthropogenic nitrogen inputs and riverine DIN exports from the Changjiang River basin under changing human pressures, *Global Biogeochem. Cy.*, 24(4), <https://doi.org/10.1029/2009GB003575>, 2010.

Yang, K., J. Zhu, J. Gu, L. Yu, and Z. Wang.: Changes in soil phosphorus fractions after 9 years of continuous nitrogen addition in a *Larix gmelinii* plantation, *Ann. For. Sci.*, 72(4), 435-442, 2015.

Yang, X., Shen, S.H., Ying, F., He, Q., Ali, M., Huo, W., Liu, X.C.: Spatial and temporal variations of blowing dust events in the Taklimakan Desert, *Theor. Appl. Climato.*, 125, 669-677, 2016a.

Yang, Y., R. Zhou, Y. Yan, Y. Yu, J. Liu, Z. Du, and D. Wu.: Seasonal variations and size distributions of water-soluble ions of atmospheric particulate matter at Shigatse, Tibetan Plateau, *Chemosphere*, 145, 560-567, <https://doi.org/10.1016/j.chemosphere.2015.11.065>, 2016b.

Yang, X., S. Wang, W. Zhang, and J. Yu.: Are the temporal variation and spatial variation of ambient SO₂



concentrations determined by different factors? *J. Clean Prod.*, 167, 824-836,

<https://doi.org/10.1016/j.jclepro.2017.08.215>, 2017.

Yu, H. L., He, N. P., Wang, Q. F., Zhu, J. X., Xu, L., Zhu, Z. L., Yu, G. R.: Wet acid deposition in Chinese natural and agricultural ecosystems: Evidence from national-scale monitoring, *J. Geophys. Res. Atmos.*,

121, 1-11, <https://doi.org/10.1002/2015JD024441>, 2016.

Yu, H., N. He, Q. Wang, J. Zhu, Y. Gao, Y. Zhang, Y. Jia, and G. Yu.: Development of atmospheric acid deposition in China from the 1990s to the 2010s, *Environ. Pollut.*, 231, 182-190,

<https://doi.org/10.1016/j.envpol.2017.08.014>, 2017a.

Yu, Y., S. Zhao, B. Wang, P. Fu, and J. He.: Pollution Characteristics Revealed by Size Distribution Properties of Aerosol Particles at Urban and Suburban Sites, Northwest China, *Aerosol Air Qual Re.*,

17(7), 1784-1797, 10.4209/aaqr.2016.07.0330, 2017b.

Zhai, P.M., Li, X.Y.: On climate background of duststorms over northern China, *Acta Geographica Sinica*, 58, 2003 (in Chinese).

Zhang, S.L., Yang, G.Y.: Changes of background values of inorganic elements in soils of gunagdong province, *Soils*, 1009-1014, 2012 (in Chinese).

Zhang, T., J. Cao, X. Tie, Z. Shen, S. Liu, H. Ding, Y. Han, G. Wang, K. Ho, and J. Qiang.: Water-soluble ions in atmospheric aerosols measured in Xi'an, China: seasonal variations and sources, *Atmos Res.*,

102(1), 110-119, <https://doi.org/10.1016/j.atmosres.2011.06.014>, 2011.

Zhang, X.-X., B. Sharratt, X. Chen, Z.-F. Wang, L.-Y. Liu, Y.-H. Guo, J. Li, H.-S. Chen, and W.-Y. Yang.: Dust deposition and ambient PM₁₀ concentration in northwest China: spatial and temporal variability,

Atmos. Chem. Phys., 17(3), 1699-1711, <https://doi.org/10.5194/acp-17-1699-2017>, 2017a.

Zhang, Y., J. Wei, A. Tang, A. Zheng, Z. Shao, and X. Liu.: Chemical Characteristics of PM_{2.5} during



2015 Spring Festival in Beijing, China, *Aerosol Air Qual. Res.*, 17(5), 1169-1180, 10.4209/aaqr.2016.08.0338, 2017b.

Zhang, Z., J. Gao, L. Zhang, H. Wang, J. Tao, X. Qiu, F. Chai, Y. Li, and S. Wang.: Observations of biomass burning tracers in PM_{2.5} at two megacities in North China during 2014 APEC summit, *Atmos. Environ.*, 169, 54-64, <https://doi.org/10.1016/j.atmosenv.2017.09.011>, 2017c.

Zhang, X., F. Chai, S. Wang, X. Sun, and M. Han.: Research progress of acid precipitation in China, *Res. Environ. Sci.*, 23(5), 527-532, 2010 (in Chinese).

Zhang, Y.Y., Liu, J.F., Mu, Y.J., Pei, S.W., Lun, X.X., Chai, F.H.: Emissions of nitrous oxide, nitrogen oxides and ammonia from a maize field in the North China Plain, *Atmos. Environ.*, 45, 2956-2961, <https://doi.org/10.1016/j.atmosenv.2010.10.052>, 2011.

Zhang, Y., W. Huang, T. Cai, D. Fang, Y. Wang, J. Song, M. Hu, and Y. Zhang.: Concentrations and chemical compositions of fine particles (PM_{2.5}) during haze and non-haze days in Beijing, *Atmos. Res.*, 174, 62-69, <https://doi.org/10.1016/j.atmosres.2016.02.003>, 2016.

Zhao, C., and K. Luo.: Sulfur, arsenic, fluorine and mercury emissions resulting from coal-washing byproducts: A critical component of China's emission inventory, *Atmos. Environ.*, 152, 270-278, <https://doi.org/10.1016/j.atmosenv.2016.12.001>, 2017.

Zhao, J., F. Zhang, Y. Xu, and J. Chen.: Characterization of water-soluble inorganic ions in size-segregated aerosols in coastal city, Xiamen, *Atmos. Res.*, 99(3), 546-562, <https://doi.org/10.1016/j.atmosres.2010.12.017>, 2011.

Zhao, M., S. Wang, J. Tan, Y. Hua, D. Wu, and J. Hao.: Variation of urban atmospheric ammonia pollution and its relation with PM_{2.5} chemical property in winter of Beijing, China, *Aerosol Air Qual. Res.*, 16(6), 1378-1389, 10.4209/aaqr.2015.12.0699, 2016.



Zheng, B., H. Huo, Q. Zhang, Z. Yao, X. Wang, X. Yang, H. Liu, and K. He.: High-resolution mapping of vehicle emissions in China in 2008, Atmos. Chem. Phys., 9787, <https://doi.org/10.5194/acp-14-9787-2014>, 2014.

Zhou, Y., Y. Zhao, P. Mao, Q. Zhang, J. Zhang, L. Qiu, and Y. Yang.: Development of a high-resolution emission inventory and its evaluation and application through air quality modeling for Jiangsu Province, China, Atmos. Chem. Phys., 17(1), 211-233, <https://doi.org/10.5194/acp-17-211-2017>, 2017a.

Zhou, Y., Xing, X.F., Lang, J.L., Chen, D.S., Cheng, S.Y., Wei, L., Wei, X., Liu, C.: A comprehensive biomass burning emission inventory with highspatial and temporal resolution in China, Atmos. Chem. Phys., 17, 2839-2864, <https://doi.org/10.5194/acp-17-2839-2017>, 2017b.



Figure and table caption

Fig. 1 The spatial distribution of 320 cities and five ecological regions.

Fig. 2 The inter-annual and seasonal variation of pH and EC of the precipitation in China.

Fig. 3 The spatial distribution of pH and EC of the precipitation in China.

Fig. 4 The temporal variation of water-soluble ions in the precipitation.

Fig. 5 The spatial variation of NO_3^- , NH_4^+ , and SO_4^{2-} in the precipitation.

Fig. 6 The spatial distribution of Ca^{2+} , Cl^- , F^- , K^+ , Mg^{2+} , and Na^+ in the precipitation.

Fig. 7 The triangular diagrams of NF for main alkaline ions.

Fig. 8 The EF_{sea} and EF_{soil} of NO_3^- , SO_4^{2-} , and NH_4^+ .

Fig. 9 The spatial variation of SSF, CF, and AF for NO_3^- , NH_4^+ , and SO_4^{2-} in the precipitation.

Fig. 10 The seasonal difference of contribution ratios of anthropogenic source, crustal source, and sea source.

Fig. 11 The local regression coefficient of influential factors for the NO_3^- , NH_4^+ , and SO_4^{2-} .

Tab. 1 The comparison of physicochemical properties and chemical composition in the precipitation.

Tab. 2 The mean enrichment factor relative to sea and soil, and the source contribution (%) of major ions in China (SSF denotes sea salt fraction, CF represents the crustal source, AF indicates the anthropogenic fraction).

Tab. 3 The loading matrix of precipitation in four seasons of China.

Tab. 4 The results of stepwise regression method.



Fig. 1

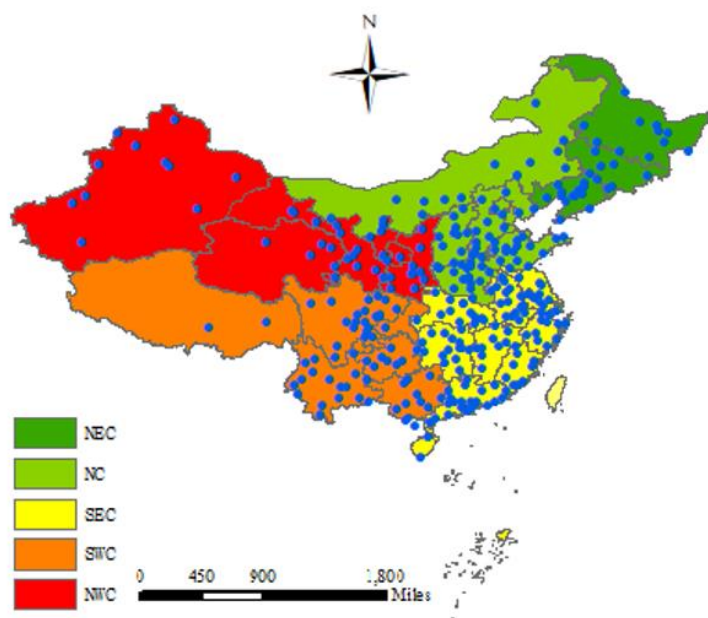




Fig. 2

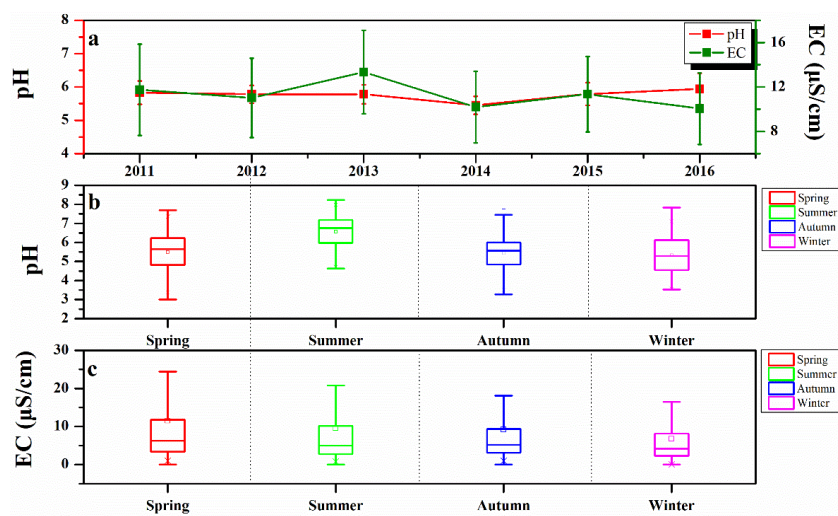




Fig. 3

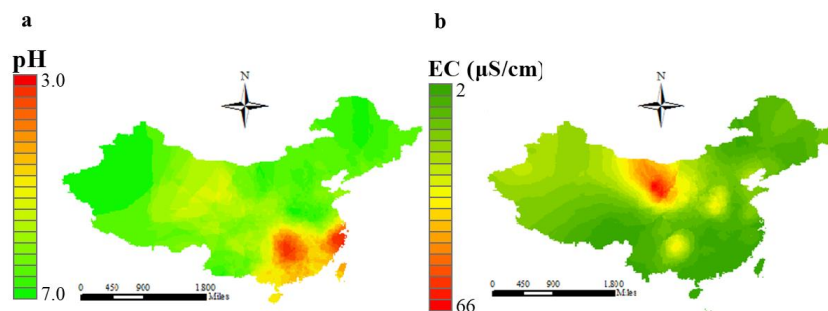




Fig. 4

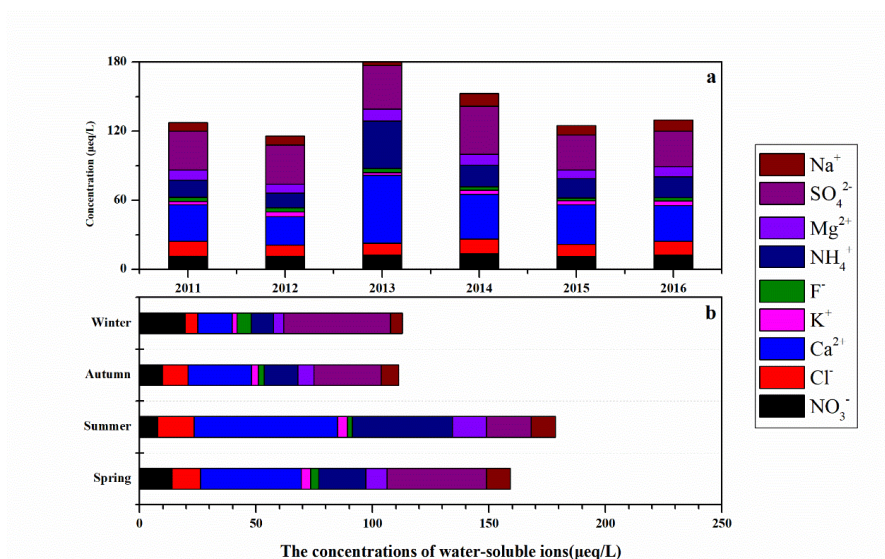




Fig. 5

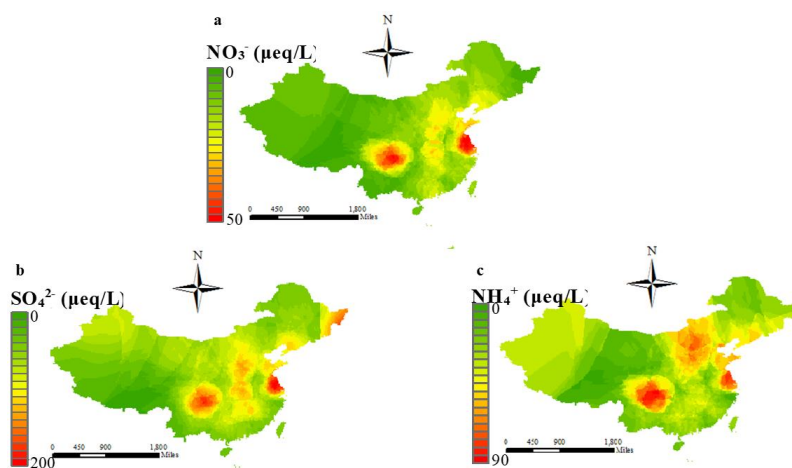




Fig. 6

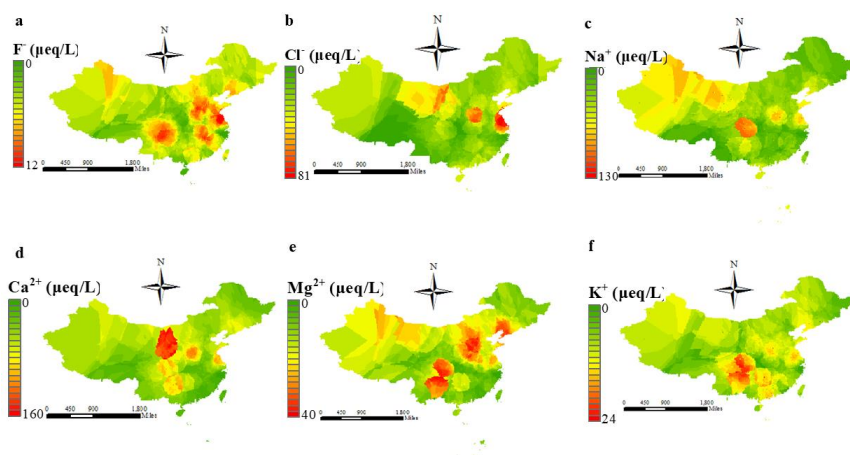




Fig. 7

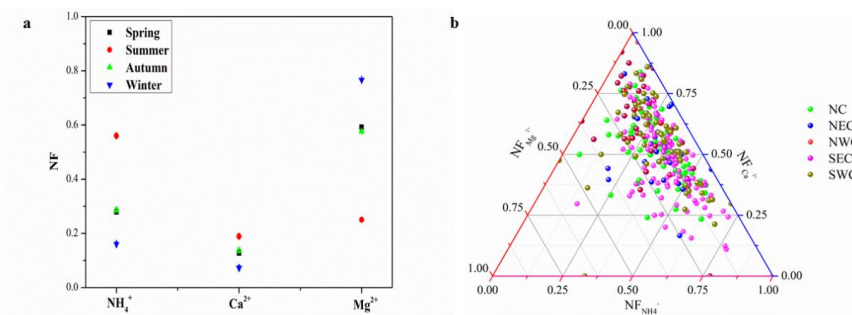




Fig. 8

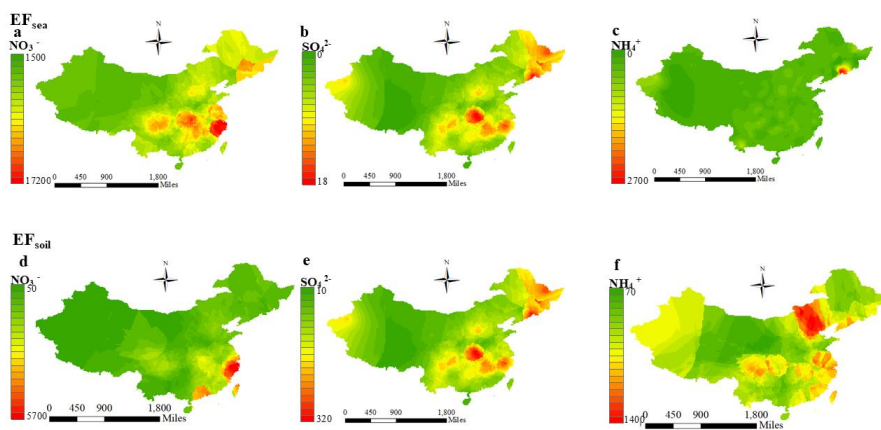




Fig. 9

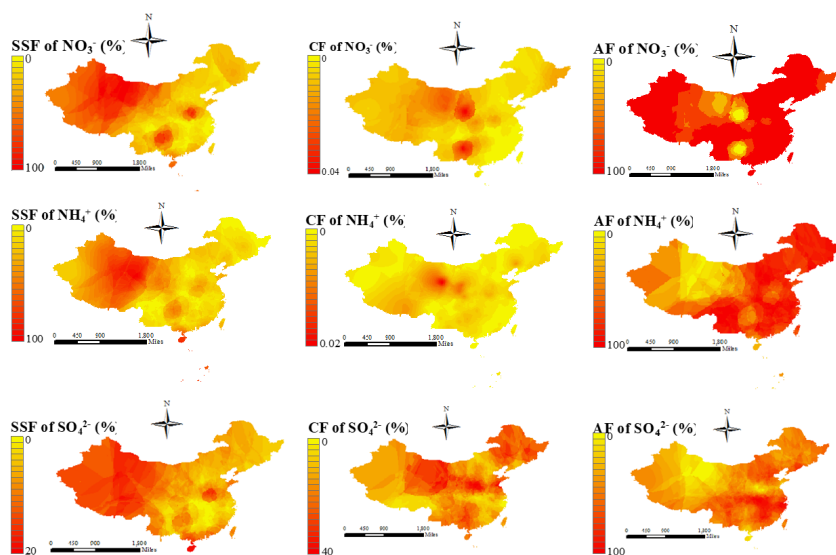




Fig. 10

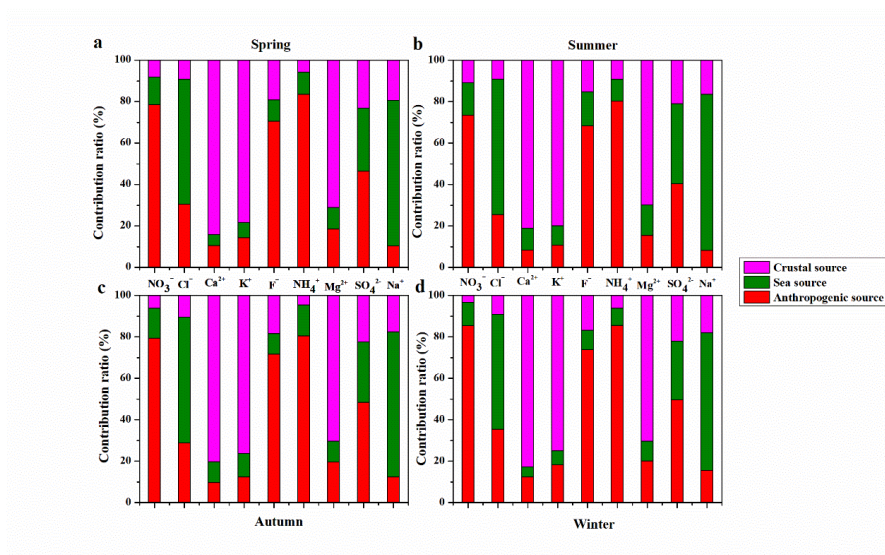
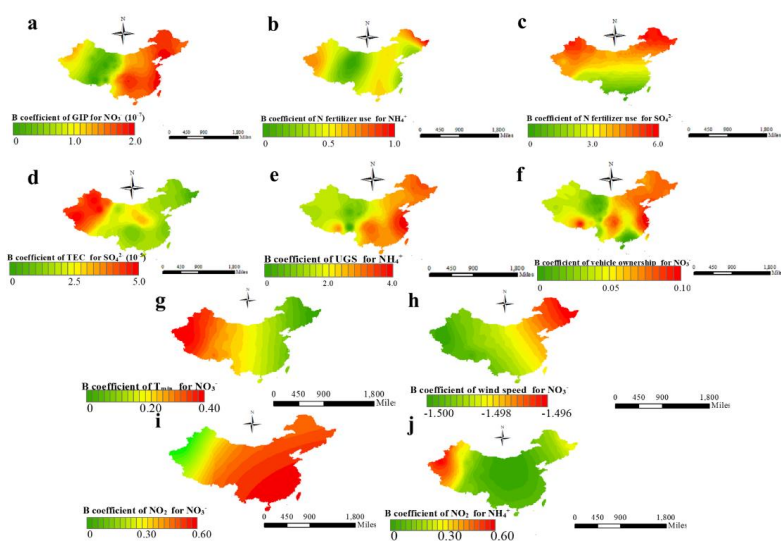




Fig. 11





Tab. 1

| | pH | EC | NO ₃ ⁻ | Cl ⁻ | Ca ²⁺ | K ⁺ | F | NH ₄ ⁺ | Mg ²⁺ | SO ₄ ²⁻ | Na ⁺ | Year | References |
|-------------|------|-------|------------------------------|-----------------|------------------|----------------|------|------------------------------|------------------|-------------------------------|-----------------|-------|--------------------------------|
| Beijing | 5.68 | 9.89 | 15.13 | 6.62 | 26.27 | 1.80 | 2.24 | 45.33 | 5.51 | 31.28 | 3.39 | 2011- | This study |
| Zhengzhou | 6.09 | 26.44 | 37.10 | 72.45 | 109.23 | 8.25 | 5.80 | 23.82 | 20.54 | 25.80 | 6.40 | 2011- | This study |
| Harbin | 6.13 | 7.41 | 9.87 | 20.71 | 21.98 | 5.02 | 5.03 | 11.96 | 9.55 | 28.76 | 22.00 | 2011- | This study |
| Shenyang | 5.76 | 8.40 | 24.52 | 15.90 | 75.32 | 2.59 | 4.32 | 40.68 | 22.68 | 57.57 | 16.88 | 2011- | This study |
| Qingdao | 5.32 | 16.53 | 5.25 | 5.79 | 28.18 | 2.07 | 1.34 | 9.28 | 9.80 | 10.96 | 25.30 | 2011- | This study |
| Shanghai | 4.39 | 2.50 | 40.06 | 4.15 | 19.09 | 1.07 | 1.45 | 17.48 | 4.71 | 29.13 | 20.36 | 2011- | This study |
| Wuhan | 4.68 | 2.66 | 11.61 | 2.12 | 13.55 | 0.76 | 1.07 | 9.38 | 2.63 | 27.93 | 1.28 | 2011- | This study |
| Guangzhou | 4.98 | 2.84 | 26.74 | 19.38 | 41.60 | 9.42 | 3.93 | 13.58 | 8.33 | 35.76 | 9.57 | 2011- | This study |
| Chengdu | 4.89 | 6.03 | 48.08 | 22.13 | 44.42 | 12.60 | 9.21 | 65.19 | 8.23 | 77.16 | 15.06 | 2011- | This study |
| Lhasa | 5.21 | 4.51 | 0.50 | 1.65 | 7.66 | 0.48 | 0.94 | 0.91 | 1.28 | 1.44 | 1.62 | 2011- | This study |
| Urumqi | 6.13 | 13.41 | 16.87 | 30.38 | 115.24 | 4.76 | 2.02 | 73.76 | 19.41 | 56.76 | 28.87 | 2011- | This study |
| Lanzhou | 5.05 | 58.06 | 16.19 | 4.93 | 51.84 | 1.24 | 1.57 | 3.05 | 8.17 | 33.30 | 10.87 | 2011- | This study |
| Jiuzhaigou | 5.95 | 15.70 | 9.10 | 44.10 | 55.80 | 34.80 | 0.86 | 18.40 | 5.60 | 15.90 | 12.60 | 2015- | Qiao et al. (2018) |
| Yulong | 5.94 | 10.30 | 4.00 | 1.96 | 37.7 | 2.46 | 1.20 | 13.20 | 5.68 | 28.30 | 3.72 | 2012 | Niu et al. (2014) |
| Nam Co | 6.59 | 19.70 | 10.00 | 19.20 | 301 | 14.50 | - | 18.10 | 7.43 | 15.50 | 15.40 | 2005 | Li et al. (2007) |
| Southern | - | - | 20.97 | 31.06 | 46.68 | 11.14 | - | 58.57 | 22.55 | 45.97 | 56.41 | 2005- | Tsai et al. (2011) |
| Petra, | 6.80 | 160 | 35.70 | 80.60 | 163.10 | 26.30 | - | 18.40 | 62.30 | 53.20 | 75.60 | 2002- | Al-Khashman et al. (2005) |
| Tokyo, | 4.52 | - | 30.50 | 55.20 | 24.90 | 2.90 | - | 40.4 | 11.5 | 50.2 | 37.0 | 1990- | Okuda et al. (2005) |
| Guaiba, | 5.92 | 10.8 | 4.00 | 13.80 | 21.50 | 5.81 | 5.90 | 38.90 | 8.85 | 23.10 | 15.10 | 2002 | Migliavacca et al. (2005) |
| Sao Paulo, | - | - | 15.60 | 0.90 | 5.50 | 3.70 | - | 27.90 | 1.70 | 8.60 | 3.60 | 2000 | Fornaro and Gutz (2003). |
| Singapore | - | - | 16.80 | 22.10 | 21.7 | 3.96 | - | 17.3 | 7.46 | 58.7 | 31.1 | 1997- | Balasubramanian et al. (2001) |
| Newark, | - | - | 14.40 | 10.70 | 6.00 | 1.30 | - | 24.40 | 3.30 | 38.10 | 10.90 | 2006- | Song and Gao (2009) |
| Patras, | 5.16 | -- | 19.40 | 114.30 | 98.50 | 6.60 | -- | 16.30 | 30.40 | 46.10 | 90.20 | 2000- | Glavas and Moschonas (2002) |
| Sardinia, | 5.18 | -- | 29 | 322 | 70 | 17 | -- | 25 | 77 | 90 | 252 | 1992- | Le Bolloch and Guerzoni (1995) |
| Adirondack, | 4.50 | -- | 22.60 | 2.14 | 3.59 | 0.33 | -- | 10.50 | 0.99 | 36.90 | 1.61 | 1988- | Ito et al. (2002) |



Tab. 2

| | EF _{sea} | EF _{soil} | SSF | CF | AF |
|-------------------------------|-------------------|--------------------|-------|-------|-------|
| NO ₃ ⁻ | 3507.49 | 59.36 | 0 | 0.02 | 99.98 |
| Cl ⁻ | 1.13 | 169.88 | 88.31 | 0.59 | 11.10 |
| Ca ²⁺ | 231.56 | 1.00 | 0.06 | 99.94 | 0 |
| K ⁺ | 16.16 | 0.83 | 4.88 | 95.12 | 0 |
| F ⁻ | 5864.28 | 9.96 | 0.02 | 10.04 | 89.94 |
| NH ₄ ⁺ | 10.51 | 86.31 | 0.10 | 0.01 | 99.89 |
| Mg ²⁺ | 10.18 | 0.55 | 2.94 | 97.06 | 0 |
| SO ₄ ²⁻ | 7.22 | 5.13 | 13.85 | 19.50 | 66.65 |
| Na ⁺ | 1.00 | 1.83 | 64.66 | 35.34 | 0 |



Tab. 3

| Season | Variable | F1 | F2 | F3 |
|---------|-------------------------------|-------------|-------------|-------------|
| Overall | NO ₃ ⁻ | 0.71 | 0.24 | 0.45 |
| | Cl ⁻ | 0.43 | 0.64 | -0.12 |
| | Ca ²⁺ | 0.42 | -0.22 | 0.75 |
| | K ⁺ | 0.39 | 0.18 | 0.72 |
| | F ⁻ | 0.68 | -0.20 | 0.45 |
| | NH ₄ ⁺ | 0.74 | 0.35 | 0.13 |
| | Mg ²⁺ | -0.41 | 0.10 | 0.66 |
| | SO ₄ ²⁻ | 0.63 | 0.23 | 0.14 |
| | Na ⁺ | -0.02 | 0.65 | 0.45 |
| Spring | NO ₃ ⁻ | 0.76 | 0.11 | -0.32 |
| | Cl ⁻ | -0.33 | 0.59 | 0.26 |
| | Ca ²⁺ | 0.32 | -0.16 | 0.80 |
| | K ⁺ | -0.36 | 0.06 | 0.78 |
| | F ⁻ | 0.70 | -0.10 | 0.20 |
| | NH ₄ ⁺ | 0.68 | 0.29 | -0.46 |
| | Mg ²⁺ | -0.38 | 0.42 | 0.69 |
| | SO ₄ ²⁻ | 0.77 | 0.31 | 0.22 |
| | Na ⁺ | -0.04 | 0.72 | 0.46 |
| Summer | NO ₃ ⁻ | 0.63 | 0.24 | -0.33 |
| | Cl ⁻ | 0.42 | 0.66 | -0.38 |
| | Ca ²⁺ | 0.44 | -0.26 | 0.85 |
| | K ⁺ | -0.37 | 0.19 | 0.70 |
| | F ⁻ | 0.54 | -0.32 | 0.48 |
| | NH ₄ ⁺ | 0.59 | 0.33 | -0.47 |
| | Mg ²⁺ | 0.32 | -0.38 | 0.60 |
| | SO ₄ ²⁻ | 0.56 | 0.36 | 0.34 |
| | Na ⁺ | -0.09 | 0.75 | 0.49 |
| Autumn | NO ₃ ⁻ | 0.73 | -0.14 | 0.38 |
| | Cl ⁻ | -0.39 | 0.62 | 0.29 |
| | Ca ²⁺ | 0.32 | -0.16 | 0.80 |
| | K ⁺ | 0.45 | -0.09 | 0.68 |
| | F ⁻ | 0.68 | -0.15 | 0.28 |



| | | | | |
|--------|-------------------------------|-------------|-------------|-------------|
| | NH ₄ ⁺ | 0.69 | 0.42 | -0.45 |
| | Mg ²⁺ | -0.29 | 0.32 | 0.71 |
| | SO ₄ ²⁻ | 0.68 | -0.29 | 0.23 |
| | Na ⁺ | -0.14 | 0.69 | -0.37 |
| Winter | NO ₃ ⁻ | 0.79 | 0.23 | -0.36 |
| | Cl ⁻ | -0.38 | 0.49 | 0.29 |
| | Ca ²⁺ | 0.39 | -0.35 | 0.65 |
| | K ⁺ | -0.39 | 0.08 | 0.72 |
| | F ⁻ | 0.75 | 0.08 | -0.24 |
| | NH ₄ ⁺ | 0.73 | 0.26 | -0.42 |
| | Mg ²⁺ | 0.35 | -0.49 | 0.75 |
| | SO ₄ ²⁻ | 0.79 | 0.22 | 0.36 |
| | Na ⁺ | -0.16 | 0.54 | 0.33 |



Tab. 4

| Dependent variables | Independent variables | Partial regression coefficients | R ² | t value | p value |
|-------------------------------|-----------------------|---------------------------------|----------------|---------|---------|
| NO ₃ ⁻ | GIP | 8.42×10 ⁻⁸ | 0.62 | 4.03 | 0.00 |
| | Vehicle ownership | 0.03 | | -2.39 | 0.01 |
| | NO ₂ | 0.34 | | 4.29 | 0.00 |
| | T _{min} | 0.15 | | 1.34 | 0.02 |
| | Wind speed | -1.49 | | -1.69 | 0.03 |
| Cl ⁻ | Dust days | 0.12 | 0.52 | 2.14 | 0.04 |
| Ca ²⁺ | PM ₁₀ | 0.36 | 0.56 | 3.26 | 0.00 |
| | Dust days | 132.74 | | 2.99 | 0.00 |
| K ⁺ | Dust days | 2.09 | 0.49 | 2.03 | 0.02 |
| F ⁻ | GIP | 0.54×10 ⁻⁷ | 0.50 | 2.31 | 0.02 |
| NH ₄ ⁺ | N fertilizer use | 0.14 | 0.48 | 2.46 | 0.02 |
| | UGS | 1.33×10 ⁻⁴ | | 1.79 | 0.04 |
| | NO ₂ | 0.25 | | 1.98 | 0.03 |
| Mg ²⁺ | Dust days | 2.36 | 0.43 | 1.65 | 0.05 |
| SO ₄ ²⁻ | TEC | 2.80×10 ⁻⁵ | 0.64 | 3.07 | 0.00 |
| | N fertilizer use | 3.36 | | 3.59 | 0.00 |
| Na ⁺ | Dust days | 2.46 | 0.46 | 1.69 | 0.04 |